Quaternary Research (2019), **91**, 111–131.

doi:10.1017/qua.2018.84

A review of climate reconstructions from terrestrial climate archives covering the first millennium AD in northwestern Europe

Dana F.C. Riechelmann[a,b]*, Marjolein T.I.J. Gouw-Bouman[b]

[a]Johannes Gutenberg-University Mainz, Institute of Geosciences, Johann-Joachim-Becher-Weg 21, D-55128 Mainz, Germany
[b]Utrecht University, Department of Physical Geography, Princetonlaan 8A, NL-3584 CB Utrecht, The Netherlands

(Received October 24, 2017; Accepted July 8, 2018)

Abstract

Large changes in landscape, vegetation, and culture in northwestern (NW) Europe during the first millennium AD seem concurrent with climatic shifts. Understanding of this relation requires high-resolution palaeoclimate reconstructions. Therefore, we compiled available climate reconstructions from sites across NW Europe (extent research area: 10°W–20°E, 45°–60°N) through review of literature and the underlying data, to identify supraregional climatic changes in this region. All reconstructions cover the period from AD 1 to 1000 and have a temporal resolution of ≤50 yr. This resulted in 22 climate reconstructions/proxy records based on different palaeoclimate archives: chironomids (1), pollen (6), *Sphagnum* mosses (1), stalagmites (8), testate amoebae (4), and tree rings (2). Comparing all temperature reconstructions, we conclude that summer temperatures between AD 1 and 250 were relatively high, and the period between AD 250 and 700 was characterised by colder summer conditions. The period from AD 700 to 1000 was again characterised by warmer summers. These temperature shifts occurred in the whole of NW Europe. In contrast, the compilation of precipitation reconstructions does not show a common pattern across NW Europe either as a result of a heterogeneous precipitation pattern or the lack of suitable and consistent precipitation proxies.

Keywords: Palaeoclimatology; Dark Ages Cold Period; Roman Warm Period; Seasonality; Temperature reconstructions; Precipitation reconstructions

INTRODUCTION

In northwestern (NW) Europe, the first millennium AD was characterised by large-scale landscape and vegetation changes, as well as significant cultural shifts. For example, in the Netherlands and Belgium, we see increased flooding in the coastal and delta region in the second half of the first millennium (e.g., Ervynck et al., 1999; Toonen, 2013; Pierik et al., 2016). On a larger scale, across NW Europe the period AD 300 to 700 is characterised by widespread forest regeneration (e.g., Germany [Kalis et al., 2008], the Netherlands [Teunissen, 1990], and the United Kingdom [Forster, 2010]). The first millennium is further defined by a strong population decline after the fall of the Roman Empire, a period known as the Migration Period, and subsequent rapid increasing population numbers during the emergence of early medieval kingdoms (e.g., Germany [Dreßler et al., 2006], France [Cheyette, 2008], and NW Europe [Wickham, 2009]). Numerous climate reconstructions from the Northern Hemisphere indicate significant climatic shifts during this time interval (Larsen et al., 2008; Ljungqvist, 2010; Wanner et al., 2011; Gräslund and Price, 2012; McCormick et al., 2012; Büntgen et al., 2016; Toohey et al., 2016), although these trends are less pronounced in global reconstructions (Rasmussen et al., 2006; Vinther et al., 2006; Wanner et al., 2008). Available climate reconstructions for the Northern Hemisphere indicate that the first millennium AD can be divided into the Roman Warm Period (AD 1–300), the Dark Ages Cold Period (AD 300–800), and the Medieval Climate Anomaly or Medieval Warm Period (AD 800–1300; Ljungqvist, 2010, and references therein).

Recent studies suggest a link between these landscape and vegetation changes, cultural shifts, and climatic variations (Tinner et al., 2003; McCormick et al., 2012; Büntgen et al., 2016; Pierik et al., 2016; Toohey et al., 2016). The extent of this influence, however, is unknown. The study of such climate impacts requires palaeoclimate reconstructions at annual to decadal resolution. However, detailed climate records covering the first millennium AD from many areas in NW Europe are at present not available.

*Corresponding author at: Johannes Gutenberg-University Mainz, Institute of Geosciences, Johann-Joachim-Becher-Weg 21, D-55128 Mainz, Germany. E-mail address: riechelm@uni-mainz.de (Dana F.C. Riechelmann).

Because the current climate in the whole of NW Europe is classified as a warm temperate, fully humid with warm summers (Cfb) after the Köppen and Geiger classification (Kottek et al., 2006), we assume that climate records from this wider region should to a larger extent reflect similar trends and thus might provide a first estimate for the climate fluctuations that occurred in regions from where climate records are not yet available.

In recent years, seven compilations of climate records have been established that include (parts of) NW Europe and cover the last two millennia. These studies, however, either cover large parts of the world or only a small region, and most compile proxy records for single climate parameters only and do not separate these into different seasons (Table 1). Thus, a review of high-resolution climate reconstructions differentiating the single climate parameters and seasons for NW Europe is still missing.

Most available climate reconstructions are based on single climate archives (e.g., chironomids, pollen, speleothems, *Sphagnum* mosses, testate amoebae, or tree rings) and/or represent small regions (Burns et al., 1998; Niggemann et al., 2003; Büntgen et al., 2005; Mangini, 2005; Wilson et al., 2005; Frisia et al., 2006; Esper et al., 2007; Litt et al., 2009; Kress et al., 2010; Barber et al., 2013). Because different proxies respond to different climatic factors and small local climate differences can occur, combining all available proxies on a continental scale may give the most complete overview of past regional climate change. In particular, terrestrial archives such as bogs, lake sediments, speleothems, and tree rings contain proxies that directly reflect climate. In addition, they allow for high-resolution reconstructions, and, therefore, they provide essential data to study short-term climate variations. To study the effects of climate on landscape, vegetation, and society, we analysed both temperature and precipitation records. Additionally, we addressed the seasonality of these climate parameters as reflected in the proxies. Helama et al. (2017a) recently recommended this approach in their worldwide compilation of climate and environmental records covering the Dark Ages Cold Period. Furthermore, we critically evaluate site- and proxy-specific errors and the accuracy of each individual chronology per studied site.

The aim of this study is to assess whether proxy records across NW Europe reflect the pattern as described previously in climate trends during the first millennium AD and to evaluate which proxies provide the most accurate reconstructions of past climate fluctuations. For this purpose, we collected and compiled the existing climate reconstructions for this region (Fig. 1, Table 2), of which we evaluate the recorded changes in temperature and precipitation, as well as their mutual consistency. We included the northern Alps in this overview because of the availability of detailed reconstructions for this region, presuming that the fluctuations shown in these records were driven by the same climate as those recorded in proxies from adjacent areas north of the Alps.

DATA COLLECTION AND DATA SETS

Data collection

The selection of climate reconstructions compiled in this study was based on the following criteria: (1) the proxy data were interpreted originally in terms of temperature or precipitation; (2) the sites are located in NW Europe or the northern Alps; (3) the records completely cover the time period of AD 1 to 1000; and (4) they have a temporal resolution of 50 yr or less. Chronological uncertainty was not a criterion for selection, because all records were dated. The chronological uncertainties range from 0 yr for tree rings and varve or layer counted chronologies to up to 520 yr 2σ-uncertainty for a ^{230}Th/U age of one speleothem. The dating uncertainties of the different records will be discussed in detail in this study. We included compiled records when (nearly) all of the individual records used in the compilation met these criteria.

The climate reconstructions were compiled from literature and, if available, downloaded from public data servers such as the database of the National Oceanic and Atmospheric Administration (NOAA, National Centers for Environmental Information; http://www.ncdc.noaa.gov/data-access/paleoclimatology-data/datasets/climate-reconstruction [accessed 18 September 2013]; http://www.ncdc.noaa.gov/data-access/paleoclimatology-data/datasets/speleothem [accessed 8

Table 1. Overview of regional and supraregional climate reconstruction review studies covering (parts of) northwestern Europe. BSi, biogenic silica; HC, historical records; NA, North Atlantic; NH, Northern Hemisphere; P, precipitation; s, summer; T, temperature; TA, testate amoebae; TOC, total organic content; TR, tree ring.

Study region	Compiled parameter	Proxy	Period	Sites in northwestern Europe	Reference
Global	T	Multiple	AD 0–2000	2	Ljungqvist (2009)
Global	Multiple	Multiple	200 BC–AD 1300	13	Helama et al. (2017a)
NH	Ts	TR	AD 800–2000	1	Wilson et al. (2016)
Extratropical NH	T	Multiple	AD 0–2000	3	Ljungqvist (2010)
High-latitude NH	T and P	Multiple	Mid–late Holocene	0	Sundqvist et al. (2010)
Eurasia	Ts	TR	AD 0–2000	1	Büntgen et al. (2016)
Europe	Ts	TR; HC	138 BC–AD 2003	1	Luterbacher et al. (2016)
British Isles and NA	T and P	Multiple	2550 BC–AD 1950	7	Charman (2010)
Iceland	T	TOC; BSi	AD 0–2000	0	Geirsdottir et al. (2009)
Ireland	T	TA	2550 BC–AD 1950	25	Swindles et al. (2013)

https://doi.org/10.1017/qua.2018.84 Published online by Cambridge University Press

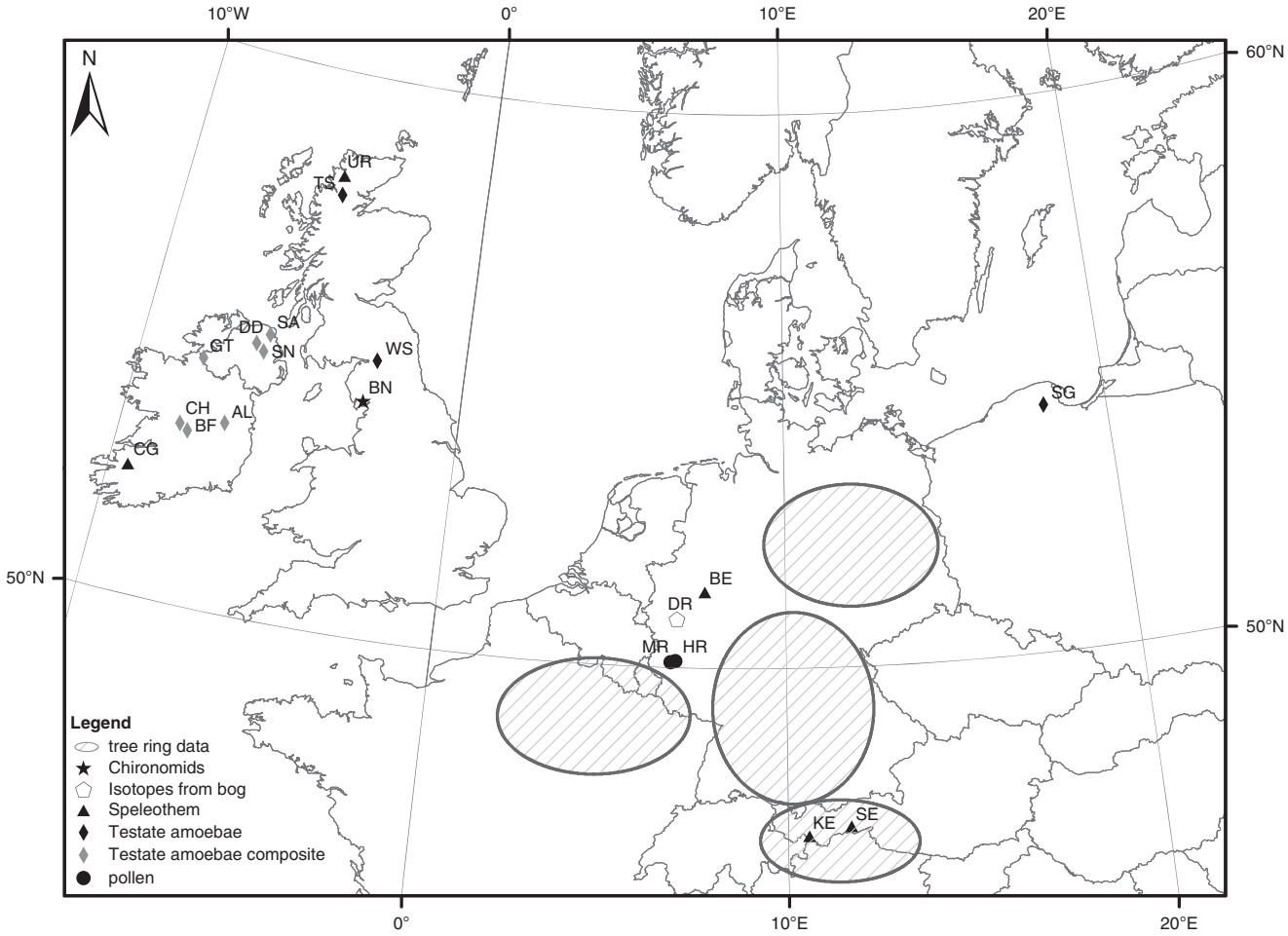

Figure 1. Map of northwestern Europe with locations of the different proxy records. See Table 2 for explanation of location codes.

December 2015]). If the data were not accessible through a public digital data repository, the authors were personally approached to provide the data series. The selected climate reconstructions are derived from (number of proxy records in parentheses) chironomids (1), pollen (6), speleothems (8), *Sphagnum* moss cellulose (1), testate amoebae (4), and tree rings (2). The records were separated into temperature and precipitation reconstructions, as well as into different seasons, using the interpretations of the related studies. For our compilation and comparison, we only used the records of inferred climate reported in previous studies; we did not reinterpret primary proxy data to a climate signal.

To enable comparison, each climate record was normalised by first subtracting the mean value of the first millennium AD and then dividing by the standard deviation of the original values covering this millennium. Furthermore, a fast Fourier transformation filter was used to perform a smoothing of the data to remove outliers and better visualise general trends. Büntgen et al. (2011) used a 60 yr smoothing filter, which was also applied to other unsmoothed records. Smoothing was not performed for records with a lower mean resolution than 25 yr. Both the normalised and smoothed data series were plotted. Shifts from warm to cold and from wet to dry were dated by defining the point where the curve crosses the AD 1 to 1000 mean value.

Uncertainties in the timing of these shifts thus depend on the dating uncertainties of the original proxy records. Subsequently, the resulting curves were compared visually. The different temperature records were subdivided into summer, winter, and annual temperature reconstructions. The precipitation records were subdivided into winter, spring, and annual precipitation reconstructions. This strategy was adopted because the selected records are both qualitative as well as quantitative records and are presented with different absolute values, some contain isotope data, some are calculated water-table depth, and others are absolute reconstructions for the different climate parameters. For qualitative records, which do not reconstruct absolute climate parameters, it is not known to what extent the amplitude of the signal reflects significant absolute temperature or precipitation shifts. If the data were compared on the basis of deviation of the mean and exceeding the standard deviation, it would be possible to under- or overestimate the climate trends.

The chronology or age-depth models of the original data sets were used to determine the end and start dates of identified climate phases. The maximum measuring error of the dates used for the construction of these age-depth models was used as an indication of the worst uncertainty in the chronology of the fluctuations. Age-depth models based on multiple dating

https://doi.org/10.1017/qua.2018.84 Published online by Cambridge University Press

Table 2. List of proxy records from terrestrial climate archives compiled in this study. AMJ, April, May, and June; DJF, December, January, and February; JJA, June, July, and August; m asl, meters above sea level.

Record	Latitude	Longitude	Altitude (m asl)	Measured proxy	Resolution of the reconstruction	Reconstructed climate parameter	Reference
Chironomids							
Bigland Tarn, England (BN)	54°14.25′ N	2°59.4′ W	160	Species assemblage	Decadal	Summer temperature	Barber et al. (2013)
Pollen							
Meerfelder Maar, Germany (MR)	50°6′ N	6°45′ E	336.5	Species assemblage	Decadal	DJF and JJA temperature, annual precipitation	Litt et al. (2009)
Holzmaar, Germany (HR)	50°7.00002′ N	6°52.99998′ E	425	Species assemblage	Decadal	DJF and JJA temperature, annual precipitation	Litt et al. (2009)
Speleothem							
Uamh an Tartair Cave, Scotland (UR)	58°8.43558′ N	4°55.81728′ W	300	Band width	Annual	Winter precipitation	Baker et al. (2015)
Crag Cave, Ireland (CG)	52°15.2028′ N	9°26.4726′ W	80	$\delta^{18}O$	Decadal	Annual temperature	McDermott et al. (2001)
Bunker Cave, Germany (BE)	53°22.05′ N	7°39.88332′ E	184	Mg/Ca ratio, $\delta^{13}C$, $\delta^{18}O$	Decadal	Winter precipitation, winter temperature, and precipitation	Fohlmeister et al. (2012)
Spannagel Cave, Austria (SE)	47°6.99198′ N	11°40.311′ E	2521	$\delta^{18}O$	Multiannual to decadal	Winter temperature	Mangini et al. (2005)
Klapferloch Cave, Austria (KE)	46°57′ N	10°33′ E	1140	$\delta^{13}C$, $\delta^{18}O$	Multiannual	Annual precipitation	Boch and Spötl (2011)
Sphagnum cellulose							
Duerres Maar, Germany (DR)	50°52.00002′ N	6°52.99998′ E	455	$\delta^{13}C$	Decadal	Growing season temperature	Moschen et al. (2011)
Testate amoebae							
Ardkill[a] (AL)	53°21.94283′ N	6°57.46758′ W	96	Species assemblage	Decadal	Annual precipitation	Swindles et al. (2013)
Ballyduff[a] (BF)	53°4.8438′ N	7°59.5506′ W	60	Species assemblage	Decadal	Annual precipitation	Swindles et al. (2013)
Cloonoolish[a] (CH)	53°11.0076′ N	8°15.0648′ W	61	Species assemblage	Decadal	Annual precipitation	Swindles et al. (2013)
Dead Island[a] (DD)	54°53.2416′ N	6°32.9328′ W	41	Species assemblage	Decadal	Annual precipitation	Swindles et al. (2013)
Glen West[a] (GT)	54°24.7134′ N	8°2.3802′ W	90	Species assemblage	Decadal	Annual precipitation	Swindles et al. (2013)
Slieveanorra[a] (SA)	55°5.1597′ N	6°11.55353′ W	290	Species assemblage	Decadal	Annual precipitation	Swindles et al. (2013)
Sluggan[a] (SN)	54°45.88428′ N	6°17.54273′ W	50	Species assemblage	Decadal	annual precipitation	Swindles et al. (2013)
Walton Moss (WS)	54°59.70937′ N	2°46.04562′ W	100	Species assemblage	Decadal	Annual precipitation	Barber and Langdon (2007)
Tore Hill Moss (TS)	57°47.55187′ N	4°51.79758′ W	-	Species assemblage	Decadal	Annual precipitation	Blundell and Barber (2005)
Stążki bog (SG)	54°25.5′ N	18°5.06663′ E	195.2	Species assemblage	Decadal	Temperature, precipitation	Galka et al. (2013)
Tree rings							
Northeastern France, northeastern/ southeastern Germany	/	/	/	Tree-ring width	Annual	AMJ precipitation	Büntgen et al. (2011)
Austrian Alps and adjacent areas	/	/	/	Tree-ring width	Annual	JJA temperature	Büntgen et al. (2011)

[a]Part of composite record.

techniques and especially absolute dating methods such as tephrochronology were assumed to be more reliable than age-depth models constructed using single dating techniques (following Swindles et al., 2013).

Data sets

Chironomids

One chironomid-inferred temperature reconstruction fulfils the requirements outlined under Data collection. This is a record from Bigland Tarn (Cumbria, UK; Fig. 1, Table 2; Supplementary Material) analysed by Barber et al. (2013), which constitutes a 5000 yr summer temperature record. The entire record was dated using 12 accelerator mass spectrometry ^{14}C dates, and the age-depth model was constructed by linear interpolation between these dates. Absolute summer temperatures were calculated using the Norwegian transfer function of Brooks and Birks (2000).

Pollen

We identified six suitable pollen-inferred climate records from two lakes in western Germany, Meerfelder Maar and Holzmaar, both located in the West Eifel volcanic field (Fig. 1, Table 2; Supplementary Material). Litt et al. (2009) collected two 10,400- and 11,000-yr-long varved records from these lakes, from which high-resolution pollen records were established. The chronologies were based on varve counting and tephrochronology and were corrected by a comparison with calibrated radiocarbon dates (Zolitschka, 1998; Brauer et al., 1999; Zolitschka et al., 2000). These two records each provide mean June, July, and August (JJA) temperature; mean December, January, and February (DJF) temperature; and annual precipitation reconstructions.

Speleothems

Speleothem records are available from Uamh an Tartair Cave (Scotland; Baker et al., 2015), Crag Cave (Ireland; McDermott et al., 2001), Bunker Cave (Germany; Fohlmeister et al., 2012), Spannagel Cave (Austria; Mangini et al., 2005), and Klapferloch Cave (Austria; Boch and Spötl, 2011). The speleothems were dated with the ^{230}Th/U method using thermal ionisation mass spectrometry or multicollector inductive coupled plasma mass spectrometry (MC-ICPMS; Richards and Dorale, 2003; Scholz and Hoffmann, 2008), as well as layer counting when annual layers occurred in the speleothems.

Uamh an Tartair cave in northwest Scotland provides a mean bandwidth record from four stalagmites (Fig. 1, Table 2; Supplementary Material; Baker et al., 2015). The bandwidths in this record show a strong negative correlation with precipitation during the period of instrumental climate data, indicating bandwidth to be a precipitation proxy. Moreover, the amount of precipitation at the location of the cave is influenced by winter North Atlantic Oscillation (NAO), making winter the dominant season for precipitation (Proctor et al., 2002).

Crag Cave in southwestern Ireland provides a palaeotemperature record based on δ^{18}O analyses of speleothem CC3 (Fig. 1, Table 2; Supplementary Material). The mean measuring resolution is 12 yr. Lower δ^{18}O values appear during colder conditions and higher δ^{18}O values during warmer conditions (McDermott et al., 2001).

Speleothems from Bunker Cave, in western Germany, provide three proxy records based on Mg/Ca ratio, δ^{13}C, and δ^{18}O measurements (Fig. 1, Table 2; Supplementary Material; Fohlmeister et al., 2012). The Mg/Ca ratio and δ^{13}C records have been measured on a single speleothem with a mean measuring resolution of 3 yr. The third proxy record is a combined record of δ^{18}O measurements, from two different speleothems, which have an average measuring resolution of 2 yr. Evapotranspiration in the summer months leads to a reduced contribution of summer rain to the water reservoir in the epikarst, resulting in a winter-dominated signal in the drip water. Furthermore, only interannual to decadal changes are recorded in the speleothems because the water is very well mixed in the epikarst (Riechelmann et al., 2011). Therefore, Mg/Ca ratios and the δ^{13}C record of the speleothem are decadal winter-dominated precipitation proxies with higher Mg/Ca ratios indicating drier conditions and vice versa. Also, the δ^{13}C record shows higher values during drier conditions, and lower values during wetter conditions. The δ^{18}O in the speleothems is a combined winter-dominated temperature and precipitation proxy, showing cold and dry conditions as high values, and warm and wet conditions as low values (Fohlmeister et al., 2012).

Spannagel Cave in the northern Austrian Alps provides a palaeotemperature record based on δ^{18}O measurements from a single stalagmite, which were measured with an average resolution of 3 yr (Fig. 1, Table 2). Based on correlations between lower alpine-winter temperatures and higher δ^{18}O values in the speleothem (and vice versa), the δ^{18}O of the speleothem has been identified as a winter temperature proxy (Mangini et al., 2005; Vollweiler et al., 2006). The age-depth model has been constructed by linear interpolation of the ^{230}Th/U dates.

Klapferloch Cave, also in the northern Austrian Alps, provides δ^{13}C and δ^{18}O records derived from one annually laminated flowstone (Fig. 1, Table 2; Supplementary Material). Correspondence on a decadal time scale is observed between changing δ^{13}C and δ^{18}O values and the amount of precipitation recorded at the nearby meteorologic station Naudes. Therefore, the δ^{13}C and δ^{18}O values of the flowstone can be used as proxies for precipitation, providing a multi-annual signal. Lower δ^{13}C and δ^{18}O values are the result of increased precipitation (and vice versa).

Sphagnum mosses

One record of $\delta^{13}C_{cellulose}$ from *Sphagnum* moss cellulose is available from Dürres Maar in western Germany (Fig. 1, Table 2; Supplementary Material; Moschen et al., 2011). This

https://doi.org/10.1017/qua.2018.84 Published online by Cambridge University Press

radiocarbon dated record has a mean resolution of 6 yr. The age-depth model was constructed by linear interpolation between the radiocarbon dates. The bog sequence covering AD 1 to 1450 completely consists of *Sphagnum capillifolium* var. *rubellum*, whereas the upper part of the core mainly contains *Sphagnum magellanicum* (Moschen et al., 2009). Both species show a dependency of their $\delta^{13}C_{cellulose}$ on growing season temperature (Ménot and Burns, 2001). Lower $\delta^{13}C_{cellulose}$ values indicate warmer conditions, and higher values point to colder conditions. The transition to higher $\delta^{13}C_{cellulose}$ values coincides with an increase in peat accumulation rate, which could be related to a high water table (Moschen et al., 2011). Therefore, reconstructed colder phases were probably also wetter phases.

Testate amoebae

Four testate-amoebae records were included in this review: single records from Scotland (Blundell and Barber, 2005), northern England (Barber and Langdon, 2007), and northern Poland (Galka et al., 2013) and a composite record from Ireland (Swindles et al., 2013).

Swindles et al. (2013) have compiled a water-table depth record based on seven testate-amoebae records from Ireland (Fig. 1, Table 2; Supplementary Material). These records are from Ardkill, Ballyduff, Cloonoolish, Dead Island, Glen West, Slieveanorra, and Sluggan. The chronologies were constructed by radiocarbon dating, multiple tephra-layer analyses, and spherical-carbon particles analyses. The testate-amoebae records were transferred to water-table depths using the European (ACCROTELM) transfer function (Charman and Blundell, 2007). Using a locally weighted regression model with bootstrapping, these single records were used to construct a best estimate, composite palaeoclimatic reconstruction.

Tore Hill Moss, a raised bog in Scotland (Fig. 1, Table 2; Supplementary Material), was analysed for macrofossils, testate amoebae, and humification rates by Blundell and Barber (2005). The chronology is based on radiocarbon dates and the Glen Garry tephra layer, which had been dated at the time of the study to 2139 ± 61 BP, corresponding to approximately AD 190 (Dugmore et al., 1995). The entire testate-amoebae record covers the period 850 BC to AD 2000. The age-depth model was based on a linear model covering the entire core, assuming a constant growth rate of the peat. Depth to water table was derived from the testate-amoebae assemblage using the transfer function of Woodland et al. (1998).

Walton Moss, an ombrotrophic bog located in northern England (Fig. 1, Table 2; Supplementary Material), was analysed by Barber and Langdon (2007). The chronology was constructed using radiocarbon dating and the Glen Garry tephra. The age-depth model was constructed by three linear regressions, which were related to changes in the macrofossil composition and possible changes in peat growth. The record covers the period 1050 BC to AD 1950. The transfer function of Woodland et al. (1998) was used to convert the testate-amoebae assemblages to bog surface wetness (BSW).

In northern Poland, one ombrotrophic bog was analysed, Stążki bog (Fig. 1, Table 2; Supplementary Material), which is a continental raised bog, differing from the aforementioned Atlantic raised bogs in NW Europe in species composition, size, and shape (Charman et al., 2009). The chronology of Stążki bog is based on radiocarbon dates and covers the period 5500 BC to AD 1250. The age-depth model has been constructed using a free-shape age-depth model fitted through the radiocarbon dates. The testate-amoebae assemblages were converted to depth to water table using the northern Poland transfer function (Lamentowicz and Mitchell, 2005; Lamentowicz et al., 2008). The clear correlation between pollen and testate amoebae in this record indicates a common forcing, probably climate (Galka et al., 2013).

Tree rings

Climate reconstructions from tree-ring width covering the period from AD 1 to 1000 are rare, in particular from NW Europe. Two reconstructions based on tree-ring width are available, one for JJA temperature from the Austrian Alps and adjacent areas and one for April, May, and June (AMJ) precipitation derived from wood from northeastern France and northeastern and southeastern Germany (Fig. 1, Table 2; Supplementary Material; Büntgen et al., 2011). The past 2500 yr JJA temperature was reconstructed from 1809 stone pine (*Pinus cembra*) and 457 European larch (*Larix decidua*) ring-width series from subfossil, historical, and living material from high-elevation sites. The past 2500 yr AMJ precipitation was reconstructed from 7284 ring-width series from subfossil, archaeological, historical, and recent oaks [*Quercus robur* L. and *Quercus petraea* (Matt.) Liebl.]. Both reconstructions were calibrated using recent meteorologic data (Büntgen et al., 2011).

RESULTS

Temperature reconstructions

Summer temperature

Five records represent summer temperature variability (Fig. 2). The proxy records cover a large part of NW Europe ranging in west–east direction from western England to western Germany and in north–south direction from central England to the Alps (Fig. 1). Except for the two pollen-inferred summer temperature records (Fig. 2c and d), all records were interpreted as reflecting summer temperature variations. The pollen-based records show minimal variations and/or no clear pattern during the period AD 1 to 1000 (Fig. 2c and d). This may be because of the low resolution of these records, 45 and 28 yr, respectively. Other contributing factors could be a low sensitivity of the pollen assemblage to small temperature changes during a relatively warm period and/or the impact of anthropogenic influences on the vegetation. The remaining records (Fig. 2a, b, and e) show similar summer temperature patterns within dating uncertainties of 80 to 190 yr, with

https://doi.org/10.1017/qua.2018.84 Published online by Cambridge University Press

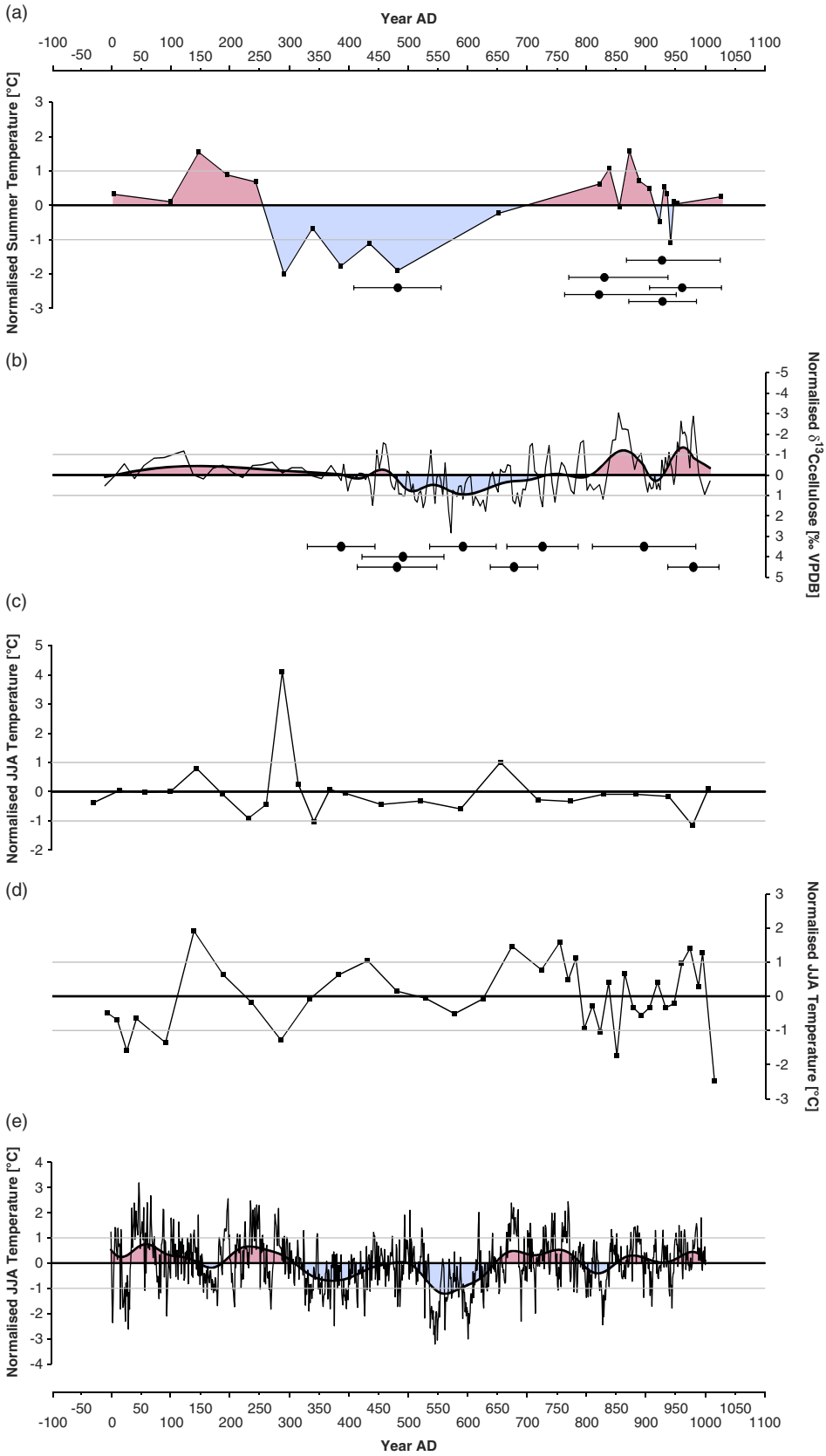

https://doi.org/10.1017/qua.2018.84 Published online by Cambridge University Press

higher summer temperatures at the start of the studied period, a change towards overall lower temperatures between AD 250 and 470, and a shift towards higher temperatures between AD 650 and 800. This is in good agreement with the starting and ending dates compiled by Helama et al. (2017a), AD 395 and AD 764 for the Dark Ages Cold Period. Around AD 930, the chironomid record (Fig. 2a) shows a second period with lower summer temperatures, which is also reflected around AD 910 in the *Sphagnum* $\delta^{13}C_{cellulose}$ record (Fig. 2b; albeit with only slightly above average values, consider the inverted y-axis). The tree-ring record from the Alps also shows a second colder period around AD 830 (Fig. 2e). The low temporal resolution of the chironomid record (about 44 yr) in addition to the overall dating uncertainties prevents accurate dating of the short colder period (Fig. 2a). Nevertheless, this chironomid record from Bigland Tarn corresponds well with two other chironomid records from Lochnagar and Talkin Tarn (Langdon et al., 2004; Dalton et al., 2005), which do not meet the criteria outlined in Data collection and, therefore, are not included in this review. The differences between the timing of the onset of the colder and the warmer periods among the different records are most probably caused by dating uncertainties in the chironomid and *Sphagnum* $\delta^{13}C_{cellulose}$ records. The chronology of the tree-ring data set is very robust, because of annual ring counting and its connection to present-day chronologies. The variations of the initiation dates are within the range of the dating uncertainties, making it likely that all records reflect the same cold period most accurately dated between AD 300 and 650 in the tree-ring data. It is, however, possible that the differences in initiation and end dates between the records are caused by an actual difference in timing and duration of this cold phase across Europe.

We can conclude that these reconstructions show warmer summer temperatures during the Roman Warm Period, colder summer temperatures during the Dark Ages Cold Period, and again warmer summer temperatures at the beginning of the Medieval Climate Anomaly (Fig. 2a, b, and e).

Winter temperature

Three records from western Germany, two pollen and one speleothem record, and one speleothem record from the northern Alps show winter temperature variability (Figs. 3 and 4). The two pollen-inferred winter temperature records do not show pronounced temperature trends in the period AD 1 to 1000 (Fig. 3a and b). However, the pollen-inferred record from Holzmaar does indicate higher winter temperatures for the period AD 1 to 250, colder conditions until AD 550, and warmer conditions until AD 1000 (Fig. 3a). The winter temperatures derived from the Meerfelder Maar pollen-based record show small anomalies in the period AD 1 to 600. From AD 600 onwards, the values show larger fluctuations, with a tendency towards higher temperatures (Fig. 3b).

The winter temperature record from Spannagel Cave is largely a reversal of the summer temperature trend. Cold conditions are inferred for AD 1 to 460 with a slightly warmer period around AD 370 (Fig. 3c). Between AD 470 and 690, winter temperatures were higher, whereas summer temperatures were lower. A second period of lower winter temperature anomalies was reconstructed for AD 690 to 800, whereas from AD 800 to 1000 reconstructed temperatures increased. This second cold phase may be coeval to a colder period in the summer temperature reconstructions dated at AD 830–900. It is also possible that the entire record is a reversal of the summer temperature and that the higher temperatures can be linked to this cold phase in summer temperature from AD 800 onwards (Figs. 2a, b, and e; 3c). The dating uncertainty of the Spannagel record is between 70 and 130 yr, making both explanations possible. The contrasting temperature pattern between summer and winter might be explained by a stronger seasonality during the Roman Warm Period with warmer summers and colder winters, followed by a lower seasonality during the Dark Ages Cold Period with colder summers and warmer winters. During the Medieval Climate Anomaly, both seasons were possibly warmer. Unfortunately, we have only one unverified record for winter temperature; therefore, its representability as a super-regional signal cannot be verified. The Spannagel record is located in the northern Alps and could therefore be influenced by a more alpine climate. Still, the high-alpine Spannagel Cave record has been linked to the NAO indicating that this record is predominantly forced by NW European climate system. The link to NAO also indicates that precipitation could have an influence on the $\delta^{18}O$ signal of the stalagmite as well (Mangini et al., 2005).

When compared to the other temperature reconstructions, the Bunker Cave $\delta^{18}O$ record shows most similarities with summer temperature reconstructions, although it is originally marked as a winter precipitation and temperature proxy (Fig. 4). The dating uncertainties of this record are very high with a minimum of 280 yr and a maximum of 520 yr. Therefore, the complete record could, in the worst case, be shifted for half of the period of interest. This record shows climatic conditions ranging from cold and dry to average conditions between AD 1 and 720. These winter climate conditions are in agreement with the winter temperature reconstruction from Spannagel Cave

Figure 2. Summer temperature reconstructions arranged from north to south. All records are normalised to the period AD 1 to 1000; 1σ standard deviations are marked with grey lines; dating points and error bars are given in the lower part of the panels. Red colour indicates warmer temperatures; and blue, colder temperatures. (a) Chironomid-based summer temperature reconstruction (Bigland Tarn, England; Barber et al., 2013). (b) Growing season temperature reconstruction from $\delta^{13}C$ of *Sphagnum* cellulose (inverse), 10 point low-pass filter (Dürres Maar, Germany; Moschen et al., 2011). (c) Pollen-based June, July, and August (JJA) temperature (Holzmaar, Germany). (d) Pollen-based JJA temperature (Meerfelder Maar, Germany; Litt et al., 2009). (e) Tree-ring–based JJA temperature, 60 yr low-pass filter (Austrian Alps and adjacent areas; Büntgen et al., 2011). VPDB, Vienna Pee Dee belemnite. (For interpretation of the references to colour in this figure legend, the reader is referred to the web version of this article.)

https://doi.org/10.1017/qua.2018.84 Published online by Cambridge University Press

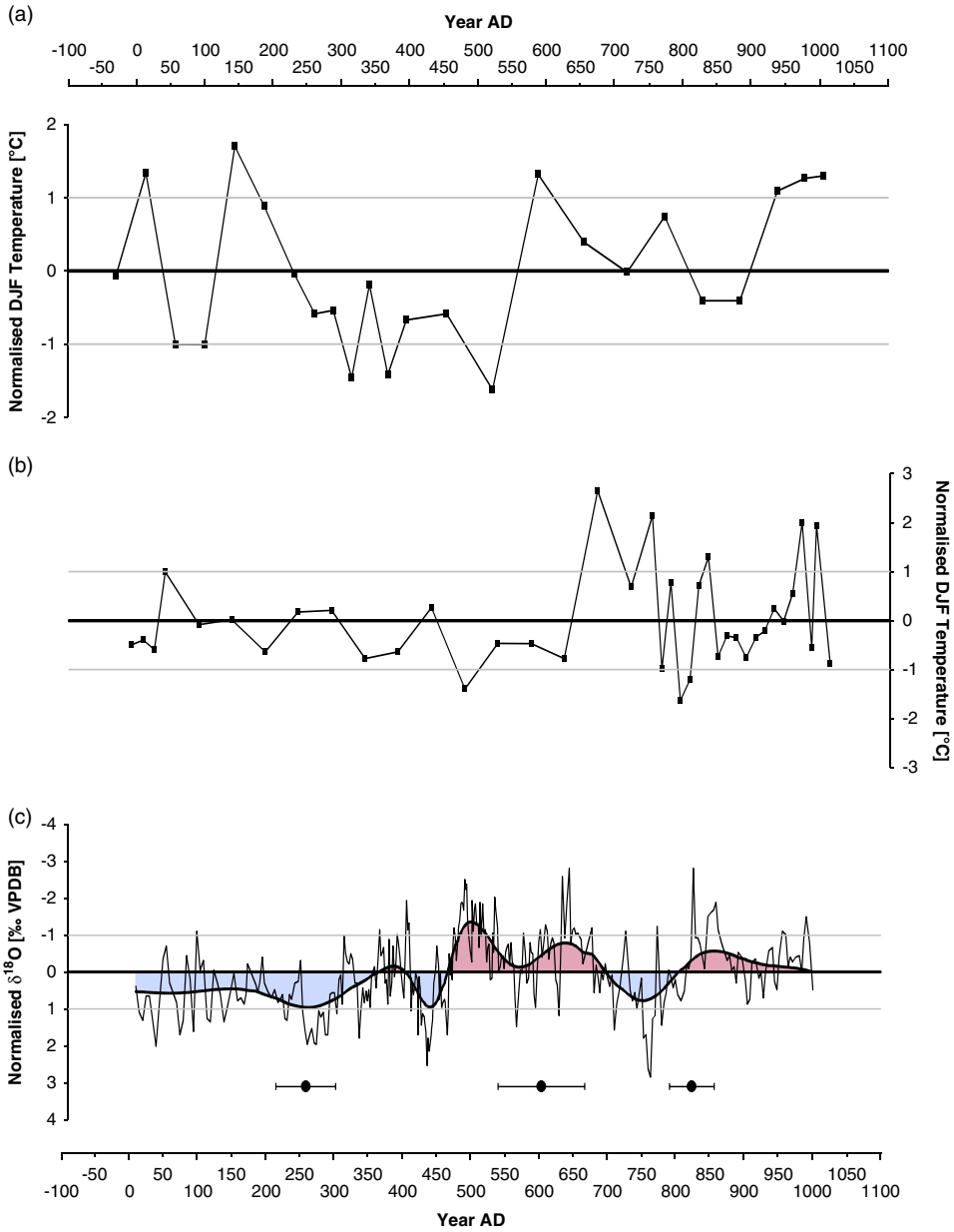

Figure 3. Winter temperature reconstructions arranged from North to South. All records are normalised to the period AD 1 to 1000; 1σ standard deviations are marked with grey lines; dating points and error bars are given in the lower part of the panel. Red colour indicates warmer temperatures; and blue, colder temperatures. (a) Pollen-based December, January, and February (DJF) temperature (Holzmaar, Germany). (b) Pollen-based DJF temperature (Meerfelder Maar, Germany; Litt et al., 2009). (c) $\delta^{18}O$ record of a speleothem (inverse), 20-point low-pass filter (Spannagel Cave, Austrian Alps; Mangini et al., 2005). VPDB, Vienna Pee Dee belemnite. (For interpretation of the references to colour in this figure legend, the reader is referred to the web version of this article.)

(Figs. 3c and 4; Mangini et al., 2005). The change to warm and wet climate conditions around AD 720 is in good agreement with the summer temperature reconstructions (Figs. 2a, b, and e; 4). The short cold and dry period around AD 900 is also visible in the summer temperature reconstructions (Fig. 2a, b, and e). A lagging effect, in addition to the dating uncertainties, in the speleothem record of Bunker Cave is possible because of buffering and mixing of the rainwater signal in the epikarst (Riechelmann et al., 2011, 2013). However, the dating uncertainties for this record are substantial, which hampers a detailed correlation to the other records.

The winter temperature records are not conclusive and either may confirm the trends in the summer temperature records or point to a reversal.

Annual temperature

The $\delta^{18}O$ record of the speleothem from Crag Cave in Ireland (McDermott et al., 2001) is considered as a proxy for annual temperature variability. This record agrees well with the summer temperature pattern with a cold phase from AD 70 to 770 and a slightly warmer period around AD 400 (Figs. 2a, b,

https://doi.org/10.1017/qua.2018.84 Published online by Cambridge University Press

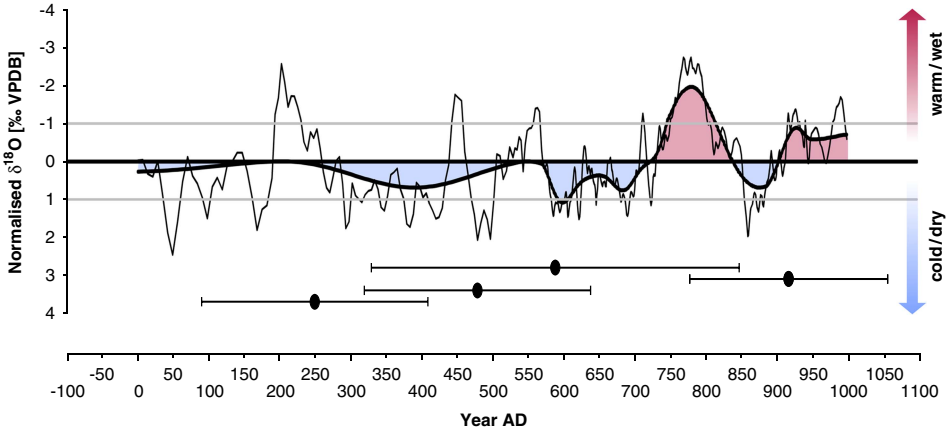

Figure 4. Winter temperature and precipitation reconstruction. The record is normalised to the period AD 1 to 1000; 1σ standard deviations are marked with grey lines; dating points and error bars are given in the lower part of the panel. Red colour indicates warm and wet conditions; and blue, cold and dry conditions. $\delta^{18}O$ record of two speleothems (inverse), 30-point low-pass filter (Bunker Cave, Germany; Fohlmeister et al., 2012). VPDB, Vienna Pee Dee belemnite. (For interpretation of the references to colour in this figure legend, the reader is referred to the web version of this article.)

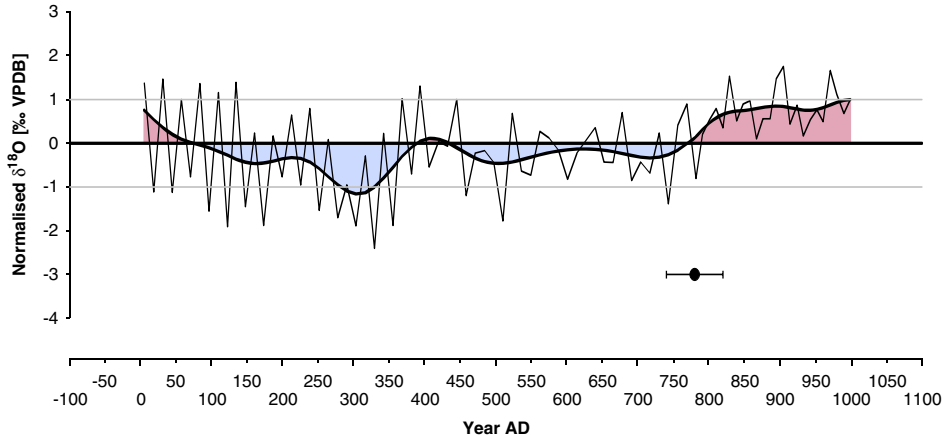

Figure 5. Annual temperature reconstruction. The record is normalised to the period AD 1 to 1000; 1σ standard deviations are marked with grey lines; dating point and error bars are given in the lower part of the panel. Red colour indicates warmer temperatures; and blue, colder temperatures. $\delta^{18}O$ record from a speleothem, 5-point low-pass filter (Crag Cave, Ireland; McDermott et al., 2001). VPDB, Vienna Pee Dee belemnite. (For interpretation of the references to colour in this figure legend, the reader is referred to the web version of this article.)

and e; 5). The onset of the colder period occurs approximately 200 yr earlier in the record from Crag Cave compared with the summer temperature reconstructions. This might be because of poor age control, with only one dating point available in this part of the speleothem record. Another cause of this difference might be that this cold phase started earlier in Ireland than for example in western Germany (Fig. 2b) and the Alps (Fig. 2e). This is, however, contradicted by the chironomid record from England, which shows the onset of the cold phase only slightly earlier at AD 250, which is in the range of age uncertainty of the other summer temperature reconstructions (Fig. 2b and e). The end of the cold phase and the change to warmer conditions at AD 780 is placed later than the summer temperature reconstructions. Although a later end date was also found in winter temperature reconstructions from the stalagmite records of Spannagel Cave in Austria (Fig. 3c) and Bunker Cave in Germany (Fig. 4), the temperature record from Crag Cave shows large variations and only a slight decrease in temperature with a distinct drop at AD 240 to 380. The temperature record from Crag Cave might be influenced by local factors and therefore does not represent a supraregional temperature signal explaining the deviation in timing and amplitude compared with the other reconstructions.

We conclude that the overall changes in reconstructed annual temperature agree with those of the summer temperatures. The differences in the timing of the onset of cold and warm phases are most probably because of the poor age control of this record.

Precipitation reconstructions

Winter precipitation

Three speleothem records were interpreted as showing winter precipitation variability (Fig. 6). The record from Scotland

https://doi.org/10.1017/qua.2018.84 Published online by Cambridge University Press

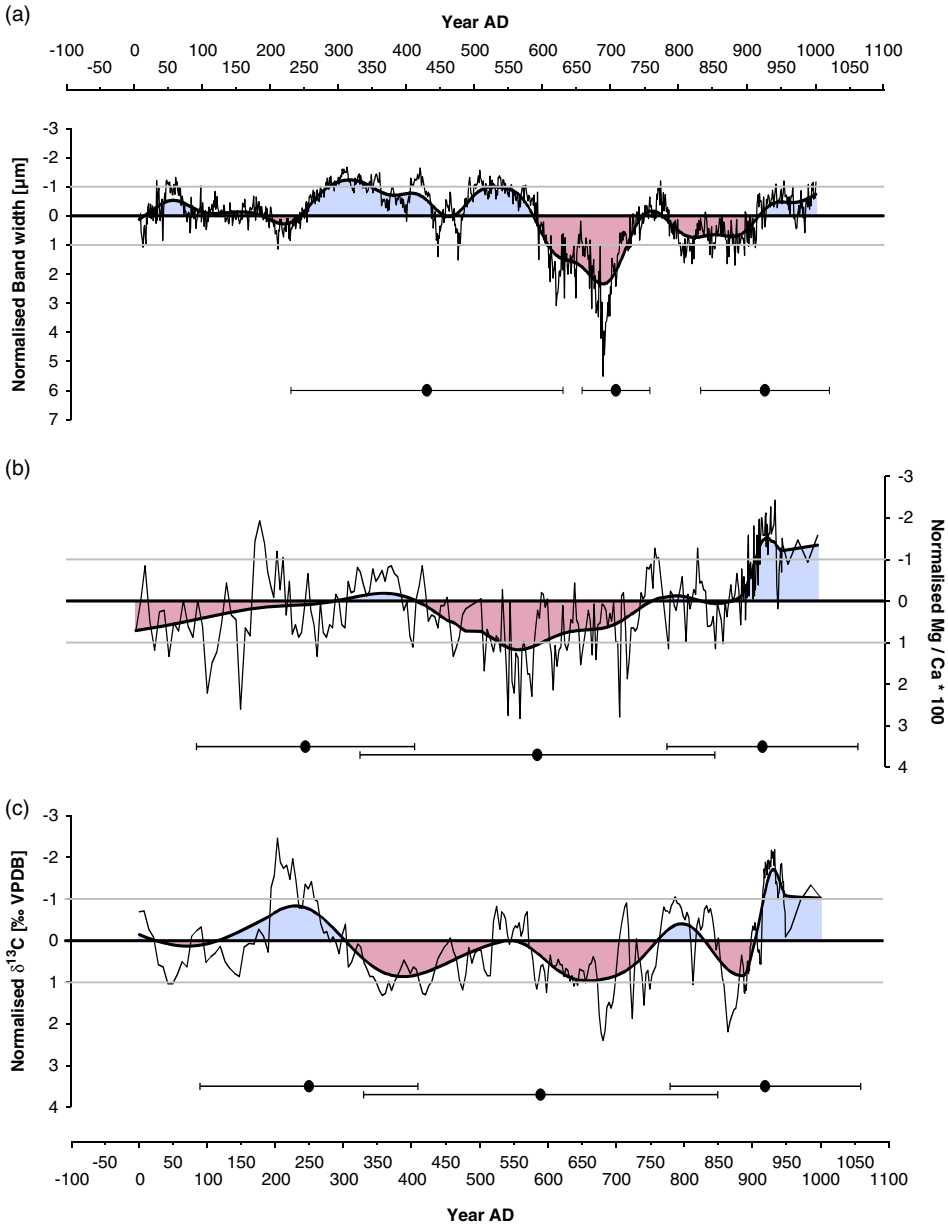

Figure 6. Winter precipitation reconstructions from west to east. The records are normalised to the period AD 1 to 1000; 1σ standard deviations are marked with grey lines; dating points and error bars are given in the lower part of the panel. Red colour indicates dry conditions; and blue, wet conditions. All records are inverse. (a) Band width record smoothed with a 60 yr low-pass filter of four speleothems (Uamh an Tartair, Scotland; Baker et al., 2015). (b) Mg/Ca-ratio record smoothed with a 20-point low-pass filter of a speleothem. (c) $\delta^{13}C$ record smoothed with a 20-point low-pass filter of a speleothem (both Bunker Cave, Germany; Fohlmeister et al., 2012). VPDB, Vienna Pee Dee belemnite. (For interpretation of the references to colour in this figure legend, the reader is referred to the web version of this article.)

(Fig. 6a) shows precipitation conditions fluctuating around average values from AD 1 to 240. Afterwards, a pronounced wet phase from AD 240 to 580 is observed, which is followed by a dry phase from AD 580 to 910 (Fig. 6a). The dry phase is interrupted by a wetter spell from AD 740 to 770. Wetter conditions were reconstructed again from AD 910 to 1000. The age control of this record is very robust because of layer counting, despite the maximum uncertainty of 402 yr in the ^{230}Th/U dating (Fig. 6a).

The two records from the same stalagmite of Bunker Cave were originally interpreted as showing the same precipitation signal, whereas the smoothed curves show some contradicting patterns (Fig. 6b and c). The Mg/Ca record is interpreted as showing drier conditions from AD 1 to 300, whereas a wet phase (based on a lower Mg/Ca ratio, please consider the inverse y-axis) around AD 190 is not represented in the smoothed curve of the Mg/Ca record. This wet phase is still visible in the smoothed curve of the $\delta^{13}C$ record, where this wet

https://doi.org/10.1017/qua.2018.84 Published online by Cambridge University Press

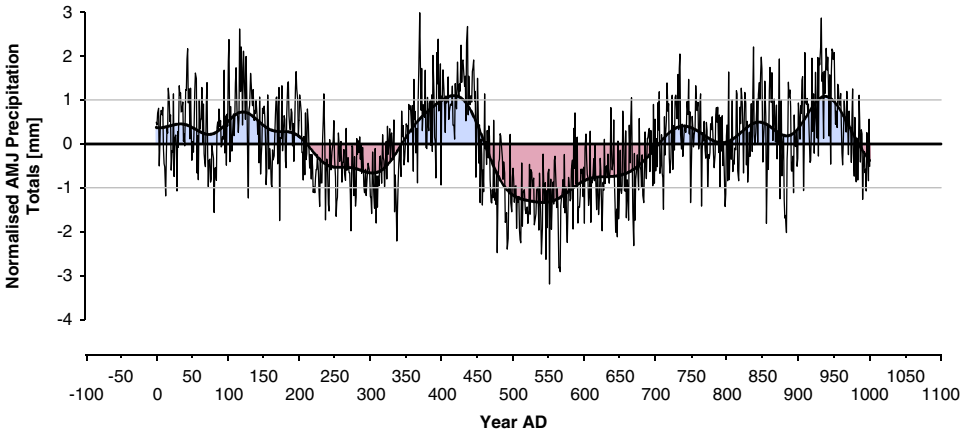

Figure 7. Spring precipitation reconstruction. The record is normalised to the period AD 1 to 1000, 1σ standard deviations are marked with grey lines. Red colour indicates dry conditions; and blue, wet conditions. April, May, and June (AMJ) precipitation reconstruction smoothed with a 60 yr low-pass filter from tree-ring width (eastern France, eastern and southern Germany; Büntgen et al., 2011). (For interpretation of the references to colour in this figure legend, the reader is referred to the web version of this article.)

phase is visible from AD 120 to 290. Slightly wetter conditions were interpreted between AD 300 and 400 in the Mg/Ca record. A pronounced dry phase occurs between AD 400 to 760 in the Mg/Ca record and between AD 300 and 760 in the $\delta^{13}C$ record. Between AD 760 and 900, both records show fluctuations around the average, and from AD 900 onwards, both records indicate wetter conditions. The dating uncertainties for these records are, with a minimum of 280 yr and a maximum of 520 yr, rather large. Despite these dating uncertainties, the overall trends of these records correspond with the record from Scotland, where average to wetter conditions were identified between AD 1 and 580 (Fig. 6a). The following drier period is visible in all records, placed at AD 300 to 760 in Germany and AD 580 to 910 in Scotland. Additional wetter conditions (AD 740 to 770) are visible in the record from Scotland and are also indicated in the other records with lower Mg/Ca ratios and $\delta^{13}C$ values around AD 780 (consider the inverse y-axis). The last wet phase in the first millennium AD (AD 900–1000) similarly shows as good correspondence across all three records. The most probable reason for the later beginning of the dry phase in the record from Scotland is that the Uamh an Tartair Cave is covered by a bog, which causes a lag and smoothing effect, but also a higher sensitivity to dry periods (Proctor et al., 2000, 2002; Fuller et al., 2008). We conclude that the record from Scotland is the most reliable record for winter precipitation because of robust age control through layer counting and its high resolution despite the buffering of the bog above the cave.

Spring precipitation

The tree-ring width record from eastern France and eastern and southern Germany (Büntgen et al., 2011) shows AMJ precipitation (Fig. 7). This reconstruction is in relatively good agreement with the winter precipitation record from Uamh an Tartair Cave in Scotland (Figs. 6a and 7). Both records show predominantly wet conditions until AD 460 (tree-rings) and AD 580 (speleothem), respectively (Figs. 6a and 7). An additional dry phase from AD 220 to 350 in the tree-ring record is also visible in higher values (consider the inverse y-axis) around AD 210 in the speleothem record from Scotland (Baker et al., 2015). A second dry phase lasted from AD 460 to 710 in the tree-ring record, and from AD 580 to 740 in the winter precipitation record from Scotland. This lag could be because of dating uncertainties or, more probably, to smoothing because of mixing and buffering effects in the karst aquifers and the bog-related lag in the speleothem record (Proctor et al., 2000, 2002; Fuller et al., 2008). The last part of the millennium from AD 710 onwards is reconstructed as wet in the tree-ring record.

Annual precipitation

Eight records were interpreted as showing annual precipitation variability based on testate amoebae, pollen, and speleothems (Fig. 8). The two precipitation reconstructions derived from pollen from Holzmaar and Meerfelder Maar were identified as unreliable precipitation variability records for the period of AD 1 to 1000 (Fig. 8d and e). These records give a pronounced underestimation of the precipitation in recent times (Litt et al., 2009).

The two British and one Irish testate-amoebae records show contradicting patterns (Fig. 8a–c), which cannot be explained by their age uncertainties only. It is assumed that testate-amoebae records on depth to water table mainly reflect changes in precipitation. It is, however, possible that the depth to water table is determined by changes in evapotranspiration and, therefore, reflects changes in temperature as well. It was also suggested by Barber and Langdon (2007) that on longer time scales BSW was more closely controlled by temperature than by precipitation. This effect is probably stronger during warm periods when increased precipitation is counteracted by increased evapotranspiration.

The composite record from Ireland shows drier conditions from AD 1 to 500 (Fig. 8a). For the second half of the first millennium AD, this record shows wetter conditions. In the temperature reconstructions, the first period is inferred as

https://doi.org/10.1017/qua.2018.84 Published online by Cambridge University Press

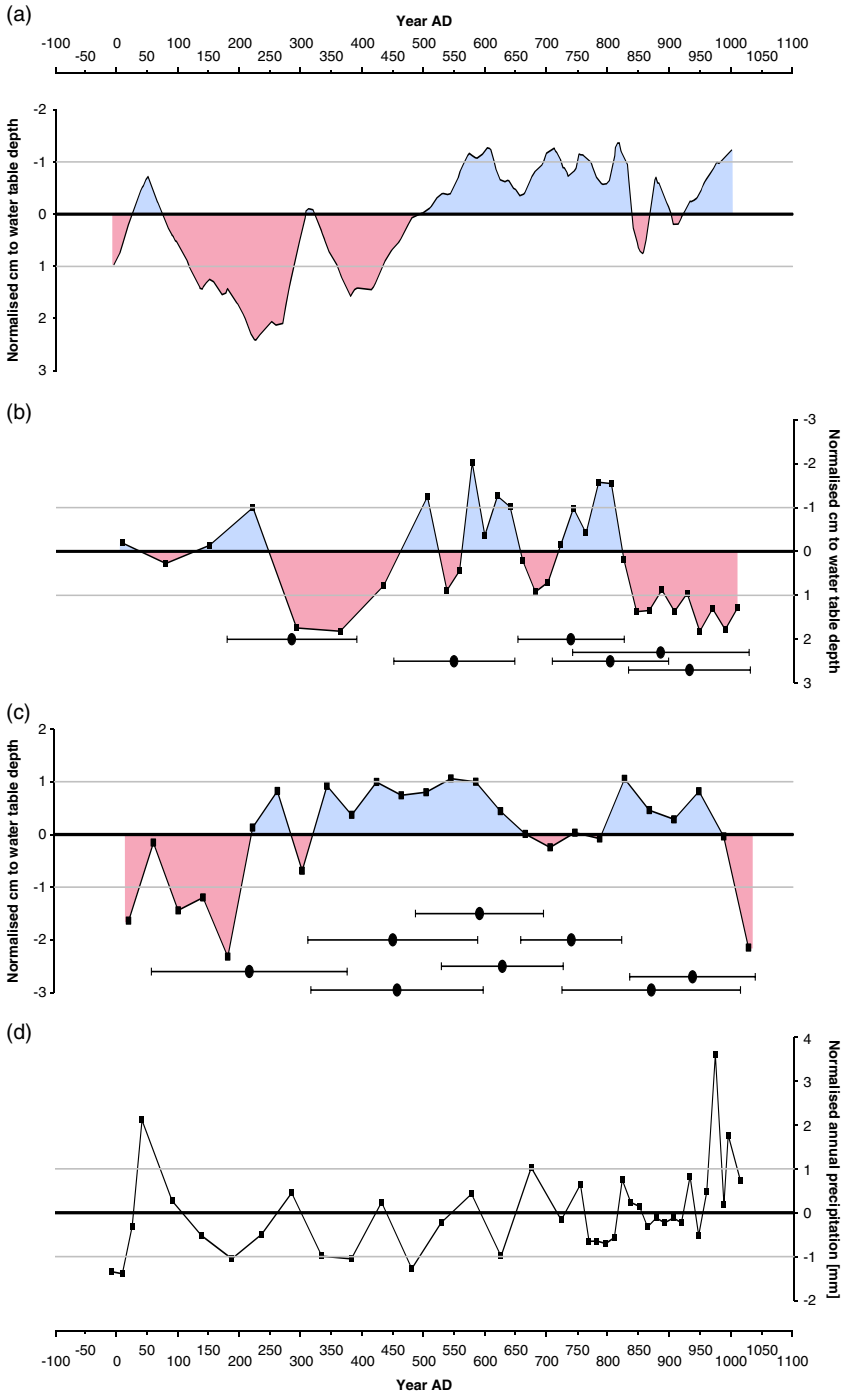

Figure. 8. (Continued)

relatively warm. The record from Walton Moss (Fig. 8c) also shows more similarities to the summer temperature reconstructions than to the other precipitation records. However, the speleothem record from Crag Cave in Ireland (Fig. 5) indicates lower temperatures, but the age control of this record is poor, with only one ^{230}Th/U age in this millennium. Therefore, a conclusion about drier and colder or warmer temperatures is not straightforward for this time period. The strong fluctuations in the record from Tore Hill Moss (Fig. 8b) might also indicate local controls or a mixed response. During the reconstructed dry phase from AD 240 to 370 in this record, there is evidence that local fires occurred. From AD 430 to 820, there are shifts to wetter conditions while the peat accumulation rate was high. The dry phase reconstructed for the period AD 240 to 370 has been correlated by Blundell and Barber (2005) to the Roman Warm Period. The period AD 430 to 820, which shows several wet shifts and overall high accumulation rates of peat, has been linked to the Dark Ages Cold Period (Blundell and Barber, 2005; Ljungqvist, 2010). The last two wet shifts in this time frame (approximately AD 540 and AD 800) are also found in other peat records in Britain and Ireland: Bolton Fell Moss

https://doi.org/10.1017/qua.2018.84 Published online by Cambridge University Press

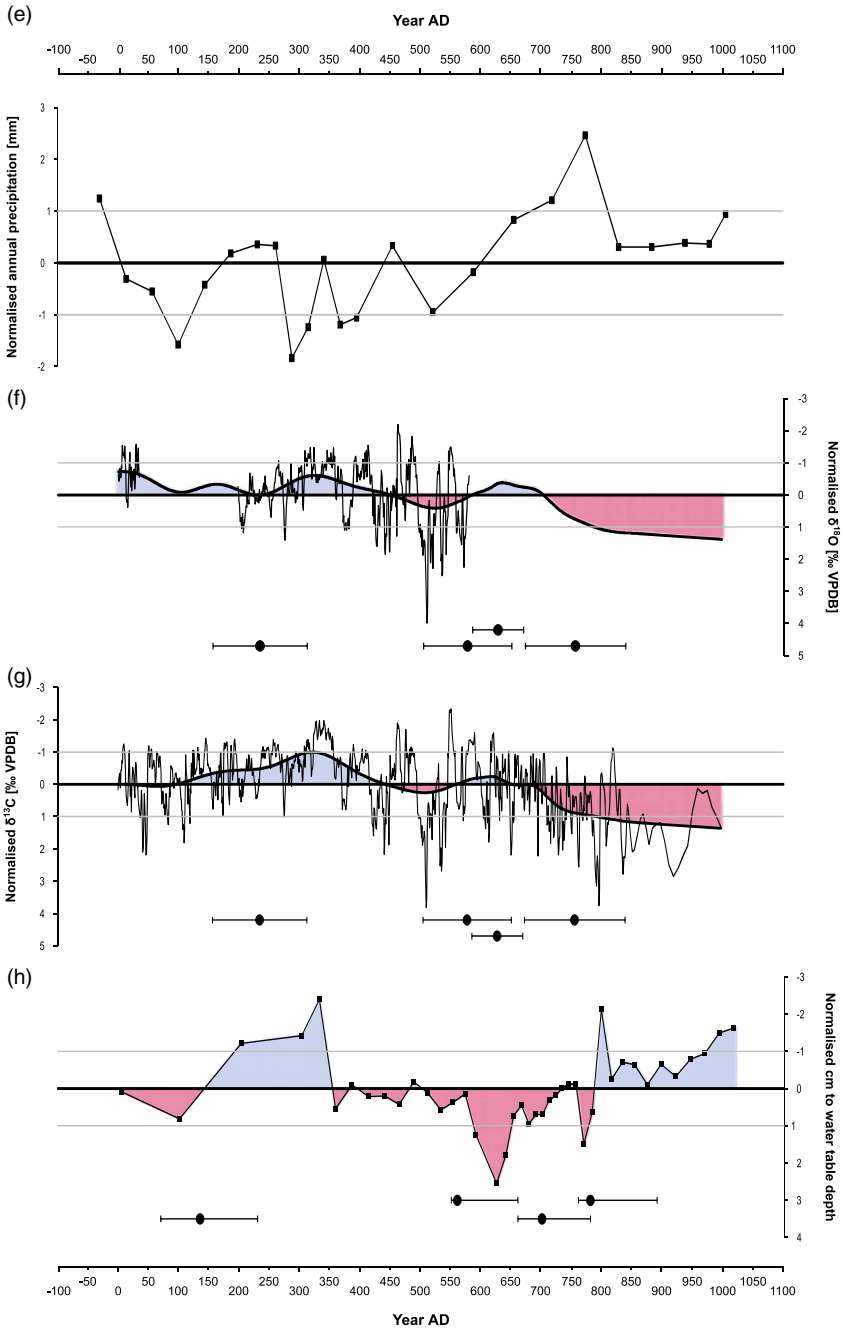

Figure 8. Annual precipitation reconstructions from west to east. The records are normalised to the period AD 1 to 1000, 1σ standard deviations are marked with grey lines; dating points and error bars are given in the lower part of the panels. Red colour indicates dry conditions; and blue, wet conditions. Records of panels a, b, f, g, and h are inverse. (a) Water-table depth reconstruction from testate amoebae (composite record, Ireland; Swindles et al., 2013). (b) Water-table depth reconstruction from testate amoebae (Torre Hill Moss, Scotland; Blundell and Barber, 2005). (c) Water-table depth reconstruction from testate amoebae (Walton Moss, England; Barber and Langdon, 2007). (d) Pollen-based annual precipitation (Meerfelder Maar, Germany). (e) Pollen-based annual precipitation (Holzmaar, Germany; Litt et al., 2009). (f) $\delta^{18}O$ record, 60 yr low-pass filter from a speleothem (Klapferloch Cave, Austria). (g) $\delta^{13}C$ record, 60 yr low-pass filter from a speleothem (Klapferloch Cave, Austria; Boch and Spötl, 2011). (h) Water-table reconstruction from testate amoebae (Stążki Bog, Poland; Galka et al., 2013). VPDB, Vienna Pee Dee belemnite. (For interpretation of the references to colour in this figure legend, the reader is referred to the web version of this article.)

(Barber, 1981), Burnfoothill Moss (Tipping, 1995), Talla Moss (Chambers et al., 1997), and Fallahogy Bog (Barber et ontinuedal., 2000; Blundell and Barber, 2005). Additional evidence for this double wet shift is found in a tree-ring record from Scandinavia (Briffa et al., 1992; Blundell and Barber, 2005). The last dry phase of the record is linked to the

https://doi.org/10.1017/qua.2018.84 Published online by Cambridge University Press

Medieval Climate Anomaly that was also recognized in Temple Hill Moss (Langdon et al., 2003; Blundell and Barber, 2005). None of aforementioned records was included separately in this review because of too low resolution for the investigated time interval (testate amoebae) or because of not covering the complete time span (tree-ring record). We conclude that especially during warm periods, the BSW or depth to water table is strongly influenced by temperature and/or other regional environmental factors; therefore, testate amoebae should be used with caution for precipitation reconstruction, which was also discussed by Charman et al. (2004).

The $\delta^{18}O$ and $\delta^{13}C$ records from Klapferloch Cave and the water-table depth reconstruction from Stążki Bog show wet climate conditions for AD 1 to 440 and AD 1 to 350, respectively (Fig. 8f–h), which corresponds well with the winter and spring precipitation reconstructions (Figs. 6a and 7). The two records from Klapferloch Cave show precipitation conditions varying around average conditions in the period AD 440 to 700 and drier conditions from AD 700 to 1000 (Fig. 8f and g). This contradicts the spring and winter precipitation reconstructions (Figs. 6a and 7). The contradicting pattern in the speleothem records from Klapferloch Cave might be because of dating uncertainties with a maximum of 170 yr and probably to buffering in the karst aquifer (Boch and Spötl, 2011). The water-table depth reconstruction from Stążki Bog further shows drier conditions from AD 350 to 790 followed by wetter conditions from AD 790 to 1000 (Fig. 8h). This corresponds, considering dating uncertainties, with the winter and spring precipitation records (Figs. 6a and 7). Therefore, this testate-amoebae record mostly seems to have been influenced by precipitation.

We conclude that some of the annual precipitation records do not contradict the patterns visible in the winter and spring precipitation records revealing a wet start of the first millennium, a drier or average middle part, and a wet last part. However, no real common spatial pattern is visible for NW Europe.

DISCUSSION

Temperature

Comparing all temperature proxies (Fig. 9), excluding the pollen-based records from Meerfelder Maar and Holzmaar, the timing of the changes differs among the reconstructions. This is most probably because of dating uncertainties in all records except the tree-ring record, with a maximum of 520 yr in the $\delta^{18}O$ record of Bunker Cave. Despite this heterogeneous pattern, some common trends can be recognised: the first millennium AD in NW Europe started with warmer summer conditions that lasted until AD 340 (+130/−90),

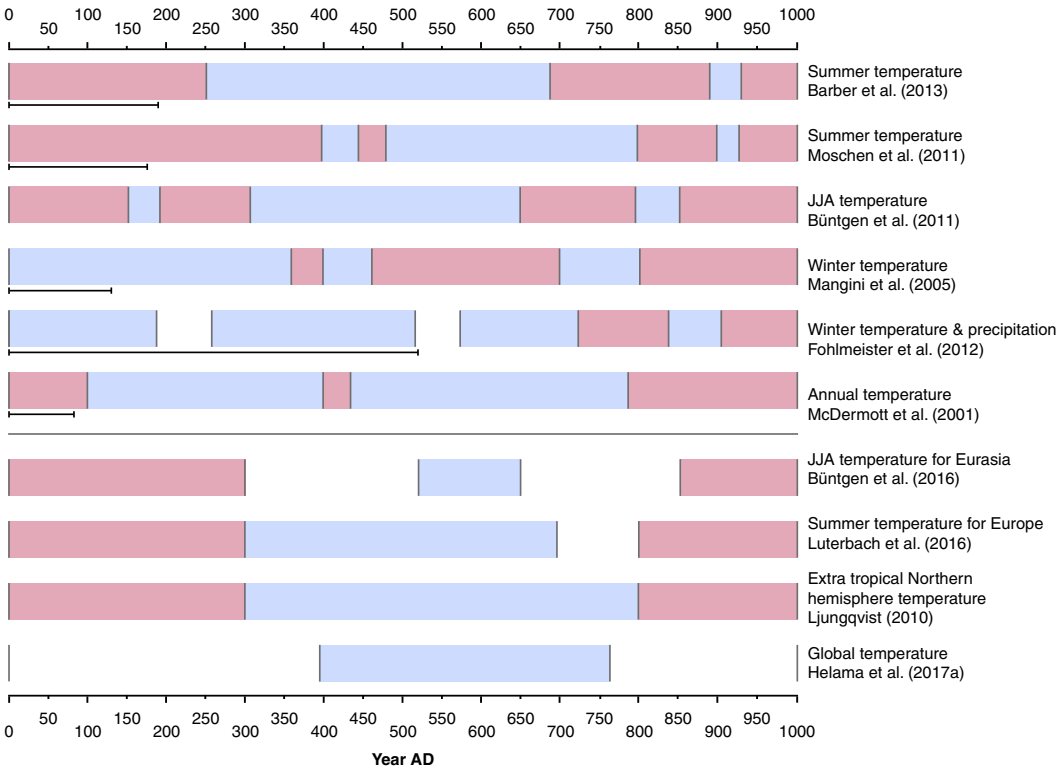

Figure 9. Comparison of the temperature records compiled in this study with the studies of Büntgen et al. (2016), Luterbacher et al. (2016), Ljungqvist (2010), and Helama et al. (2017a). Red indicates warmer conditions; blue, colder conditions; and white, average conditions. The maximum dating uncertainties are given below every record interpretation. The dating uncertainty for the tree-ring records is zero. (For interpretation of the references to colour in this figure legend, the reader is referred to the web version of this article.)

https://doi.org/10.1017/qua.2018.84 Published online by Cambridge University Press

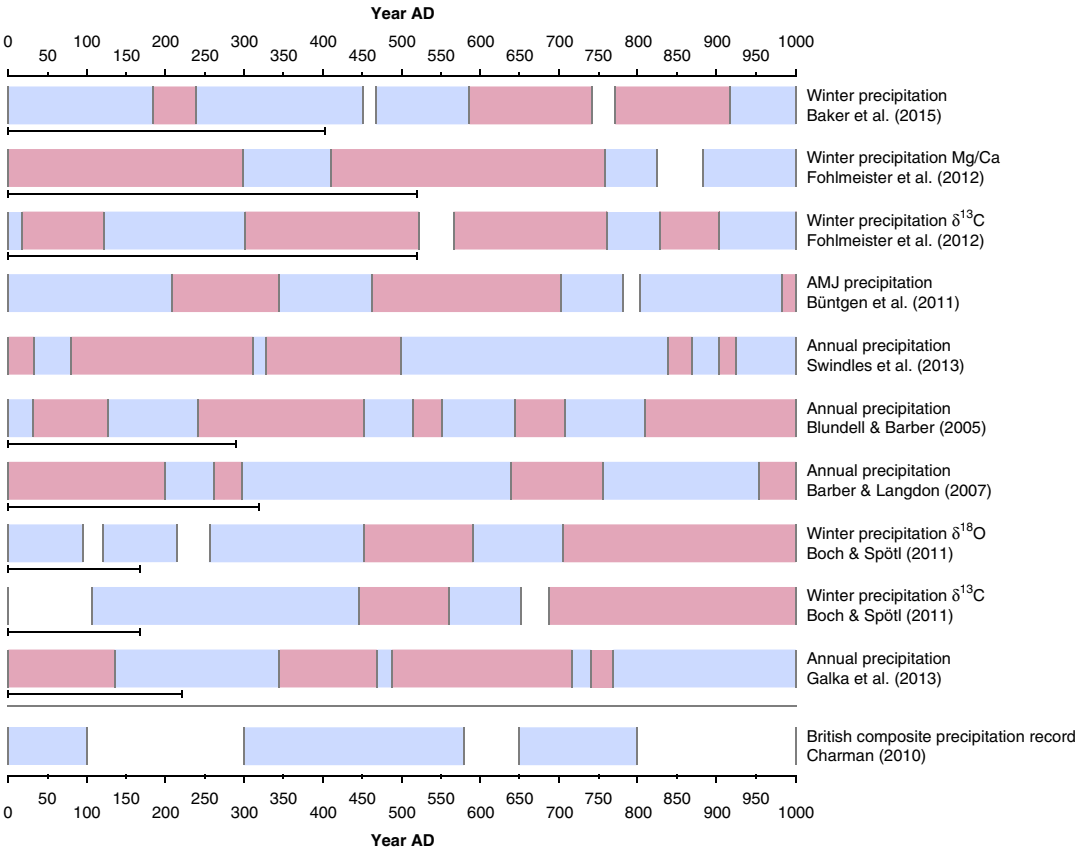

Figure 10. Comparison of the precipitation records compiled in this study with the study of Charman (2010). Red indicates drier conditions; blue, wetter conditions; and white, average conditions. The maximum dating uncertainties are given below every record interpretation, except for Swindles et al. (2013), where no dating uncertainty was provided for the composite record. (For interpretation of the references to colour in this figure legend, the reader is referred to the web version of this article.)

followed by colder conditions, which prevailed until AD 720 (+80/−70), and followed again by warmer conditions for the remainder of the first millennium AD (Fig. 9). The starting and ending of the colder period fits quite well with the findings of Helama et al. (2017a), with AD 395 to AD 764 based solely on climate records, and also with the study of Ljungqvist (2010), who defined the Roman Warm Period from AD 1 to 300, the Dark Ages Cold Period from AD 300 to 800, and the Medieval Climate Anomaly from AD 800 to 1300 for the extratropical Northern Hemisphere (Fig. 9). Büntgen et al. (2016) defined the Late Antique Little Ice Age from AD 536 to around AD 660 (Fig. 9). This very pronounced cold phase within the Dark Ages Cold Period is visible in tree-ring width records from the Alps, which is also included in this review (Fig. 2e), and an additional tree-ring width record from the Altai Mountains. However, this very cold phase is not visible in the chironomid record (Barber et al., 2013) and in the speleothem records from Ireland and the Alps (Figs. 2a, 3c, and 5; McDermott et al., 2001; Mangini et al., 2005). A more pronounced cold phase during this time is recorded in the *Sphagnum* $\delta^{13}C$ record (Fig. 2b), whereas cold and dry conditions were derived from the $\delta^{18}O$ record of Bunker Cave (Moschen et al., 2011; Fohlmeister et al., 2012). However, because of dating uncertainties and/or low resolution of these records, a precise conclusion about the Late Antique Little Ice Age is not possible. This was also shown by Helama et al. (2017b) in an overview of tree-ring records from the Northern Hemisphere where no clear Late Antique Little Ice Age was visible.

It has to be taken into account that 18 out of the 30 compiled climate records in the study of Ljungqvist (2010) represent summer temperature. There is only one record (Spannagel Cave) included in both our review and in the study of Ljungqvist (2010), so the findings are based on predominantly different data sets. The study from Helama et al. (2017a) compiled 114 multiple proxy records for different climatic parameters worldwide, but the timing of the Dark Ages Cold Period is quite consistent for all. Out of a total of 13 sites in NW Europe, 5 sites—namely, Uamh an Tartair Cave (Baker et al., 2015), Crag Cave (McDermott et al., 2001), Klapferloch Cave (Boch and Spötl, 2011), Alpine tree-ring width (Büntgen et al., 2011), and the composite record from Ireland (Swindles et al., 2013)—are included as well in our review. The agreement with the studies of Luterbacher et al. (2016) and Büntgen et al. (2016) showing summer temperature for Europe and Eurasia, respectively, also corresponds well with our findings (Fig. 9). This is partly because the same tree-ring data set has been considered in their reconstruction and the present compilation. Also, the record of McDermott et al. (2001) shows a similar pattern.

https://doi.org/10.1017/qua.2018.84 Published online by Cambridge University Press

The present data do not allow for decisive conclusions about the exact timing and duration of colder and warmer periods, which was also discussed by Helama et al. (2017a) for the Dark Ages Cold Period. This could primarily be resolved by improving the chronologies of existing and new records by independent and absolute dating such as tephra or a high number of precise ^{230}Th/U dating by MC-ICPMS and layer counting. This is important with regard to the relation of climatic changes and changes in human societies. Further, the quantitative reconstruction of the temperature remains complex, and therefore, a precise conclusion about extreme cold periods such as the Late Antique Little Ice Age (Büntgen et al., 2016) is difficult to establish. Based on the current state of research, it is impossible to identify leads and lags in spatial trends. However, we can conclude that the temperature shifts occurred across NW Europe making this a supraregional trend.

Precipitation

Three out of the 10 records interpreted as precipitation show a similar pattern, which is not as distinct as it is for temperature (Fig. 10). The remaining seven records show highly variable and often inverse patterns. We conclude that because most of these records are based on proxies that also are influenced by temperature and other environmental factors, and often by multiple factors simultaneously, they are unsuitable as pure precipitation proxies. Looking at the three most reliable records (speleothem: Uamh an Tartair Cave/Scotland; tree-ring width: France/Germany; testate amoebae: Stążki bog/Poland), we can tentatively indicate that the period from AD 1 to 500 (–150/+80) was relatively wet, whereas from AD 500 onwards drier conditions are indicated followed by wetter conditions from AD 800 (–90/+210) onwards. These climatic shifts probably have been dated most accurately in the tree-ring records, where they are visible at AD 460 and AD 710. The speleothem and tree-ring records indicate the occurrence of an additional drier phase around AD 210/220. The timing of the shifts in precipitation does not seem concurrent with the timing of the shifts in temperature. The shift to wetter conditions at the end of the first millennium could be synchronous to the start of the Medieval Climate Anomaly. The Dark Ages Cold Period (around AD 340) does not appear to be reflected in a shift in precipitation regime. Helama et al. (2017a) see evidence of a cold and wetter Dark Ages Cold Period. However, with 14 sites indicating wet conditions and 9 sites indicating dry conditions, the evidence from this study is not conclusive.

Studies compiling precipitation records from a wider area are rare. Sundqvist et al. (2010) considered precipitation but only compared mid-Holocene conditions with preindustrial times (AD 1500) and offered no significant conclusion about precipitation differences in time and space. Only the study by Charman (2010) is available for comparison with the precipitation records presented here. In that study, wet climate conditions were reconstructed from bog oaks, BSW (testate amoebae), flood layers, a speleothem from Uamh an Tartair Cave (Proctor et al., 2002), and sand dune activity. Comparing Charman's (2010) synthesis to our three precipitation records (Figs. 6a, 7, and 8h; Büntgen et al., 2011; Galka et al., 2013; Baker et al., 2015), there are only a few similarities. However, this is a common occurrence when compiling and comparing precipitation records. This is illustrated by the study of Cook et al. (2015) who reconstructed droughts during the last millennium (AD 1000 to 2000) and found no corresponding precipitation trend over NW Europe, except during for some extreme years.

The British compilation indicates wetter conditions in the period AD 1 to 100 as seen in the speleothem record from Scotland and the tree-ring reconstruction. Furthermore, this composite record points to wetter conditions in the interval AD 300 to 570 as seen in the speleothem record from Scotland (Fig. 10). Furthermore, the composite record by Charman (2010) is primarily based on BSW records from testate amoebae. One testate-amoebae record (Ballyduff) from this study was included in the composite testate-amoebae record discussed in our review. It should be noted that testate amoebae as a proxy for precipitation has to be used with caution. Furthermore, proxies reflecting solely precipitation are rare; most proxies are to some extent influenced by other environmental factors with temperature as the dominant secondary influence. It is therefore, difficult to reconstruct precipitation in isolation from temperature. Nevertheless, the tree-ring record covering large parts of Germany and eastern France (Büntgen et al., 2011) and the speleothem record from Scotland (Baker et al., 2015) seem to provide reliable precipitation reconstructions. Both are annually resolved and have excellent age control because of layer or ring counting. These records come from completely different parts of NW Europe making it likely that these shifts occurred also across the whole of this region. Our study clearly shows that precipitation shifts are poorly reflected in proxy records, probably because of low sensitivity of the proxy to precipitation and strong regional precipitation differences. More high-resolution, precisely dated records and precipitation-seasonality proxies are needed to provide conclusive evidence about the timing and duration of dry and wet phases during the first millennium.

CONCLUSIONS

We investigated 17 single records and 1 composite record based on six different climatic proxies in order to detect similar climate variations in NW Europe during the first millennium AD. Chironomids, speleothems, *Sphagnum* mosses, and tree-ring width provide good to excellent records of past climate. However, climate records based on pollen and testate amoebae appear to be less reliable, because of low resolution (pollen) and the varying dependency on both precipitation and temperature (testate amoebae).

The period from AD 1 to 250 was relatively warm and can be correlated to the Roman Warm Period found in other reconstructions from the Northern Hemisphere. This period was followed by colder conditions lasting from AD 250 to 700, which

https://doi.org/10.1017/qua.2018.84 Published online by Cambridge University Press

can be correlated to the Dark Ages Cold Period. Warmer conditions were reconstructed from AD 700 onwards, corresponding with the Medieval Climate Anomaly.

The compilation of precipitation reconstructions yields a markedly heterogeneous pattern. Only the tree-ring width reconstruction of spring precipitation, the winter precipitation record from a speleothem from Scotland, and an annual precipitation testate-amoebae record from Poland show some indications for common changes in wetness with a wet first half of the millennium, a dry middle part, and a shift to wetter conditions at the end of the millennium. This translates to a wetter Roman Warm Period, a first wetter then drier Dark Ages Cold Period, and a wetter Medieval Climate Anomaly.

The identification of the exact timing of the shifts in precipitation and temperature is hampered by poor age control except for the two tree-ring records, where climatic shifts can be exactly dated to the year, and by the fact that in some cases the records only have a multidecadal resolution. It was therefore not possible to determine further differences in the timing and duration of the climate fluctuations across NW Europe. We can conclude that the shifts in temperature occurred across the whole of this region and are recognisable in multiple records and proxies, demonstrating that the Roman Warm Period, the Dark Ages Cold Period, and the Medieval Climate Anomaly also occurred as regional climatic events. The precipitation records indicate some similarities across NW Europe, which differ in timing from the temperature shifts.

SUPPLEMENTARY MATERIAL

To view supplementary material for this article, please visit https://doi.org/10.1017/qua.2018.84

ACKNOWLEDGMENTS

This work is part of the project "The Dark Age of the Lowlands in an interdisciplinary light: people, landscape and climate in the Netherlands between AD 300 and 1000" (The Netherlands Organisation for Scientific Research (NWO), section Humanities; 2012–2019: 360-60-110; www.darkagesproject.com). We thank the following people for providing data: F. McDermott: stalagmite CC3 from Crag Cave (Ireland); J. Fohlmeister: Bunker Cave (Germany); P. Langdon, K. Barber, and A. Blundell: Irish and British testate-amoebae data; M. Lamentowicz and M. Galka: Polish testate-amoebae data; S. Alastair Brown: chironomid data set; N. Kuhl: *Sphagnum* cellulose record. G. Swindles and J. Guiot are thanked for their useful input on selecting the correct records. W. Z. Hoek, E. Jansma, H. Middelkoop, R. L. van Lanen, and E. Stouthamer are thanked for many fruitful discussions and suggestions to this manuscript, and M. Veicht for graphic editing. ERASMUS (European Community Action Scheme for the Mobility of University Students) provided additional funding for the first author. We would like to thank S. Helama, G. Plunket, associate editor P. Langdon, and senior editor D. Booth for many useful comments and remarks on the manuscript.

REFERENCES

Baker, A., Hellstrom, J.C., Kelly, B.F.J., Mariethoz, G., Trouet, V., 2015. A composite annual-resolution stalagmite record of North Atlantic climate over the last three millennia. *Scientific Reports* 5, 10307.

Barber, K., Brown, A., Langdon, P., Hughes, P., 2013. Comparing and cross-validating lake and bog palaeoclimatic records: a review and a new 5,000 year chironomid-inferred temperature record from northern England. *Journal of Paleolimnology* 49, 497–512.

Barber, K.E., 1981. *Peat Stratigraphy and Climate Change: A Palaeoecological Test of the Theory of the Cyclic Peat Bog Regeneration*. A.A. Balkema, Rotterdam, the Netherlands.

Barber, K.E., Langdon, P.G., 2007. What drives the peat-based palaeoclimate record? A critical test using multi-proxy climate records from northern Britain. *Quaternary Science Reviews* 26, 3318–3327.

Barber, K.E., Maddy, D., Rose, N., Stevenson, A.C., Stoneman, R., Thompson, R., 2000. Replicated proxy-climate signals over the last 2000 yr from two distant UK peat bogs: new evidence for regional palaeoclimate teleconnections. *Quaternary Science Reviews* 19, 481–487.

Blundell, A., Barber, K., 2005. A 2800-year palaeoclimatic record from Tore Hill Moss, Strathspey, Scotland: the need for a multi-proxy approach to peat-based climate reconstructions. *Quaternary Science Reviews* 24, 1261–1277.

Boch, R., Spötl, C., 2011. Reconstructing palaeoprecipitation from an active cave flowstone. *Journal of Quaternary Science* 26, 675–687.

Brauer, A., Endres, C., Negendank, J.F.W., 1999. Lateglacial calendar year chronology based on annually laminated sediments from Lake Meerfelder Maar, Germany. *Quaternary International* 61, 17–25.

Briffa, K.R., Jones, P.D., Bartholin, T.S., Eckstein, D., Schweingruber, F.H., Karlén, W., Zetterberg, P., Eronen, M., 1992. Fennoscandian summers from ad 500: temperature changes on short and long timescales. *Climate Dynamics* 7, 111–119.

Brooks, S.J., Birks, H.J.B., 2000. Chironomid-inferred late-glacial and early-Holocene mean July air temperatures for Krakenes Lake, western Norway. *Journal of Paleolimnology* 23, 77–89.

Büntgen, U., Esper, J., Frank, D.C., Nicolussi, K., Schmidhalter, M., 2005. A 1052-year tree-ring proxy for Alpine summer temperatures. *Climate Dynamics* 25, 141–153.

Büntgen, U., Myglan, V.S., Ljungqvist, F.C., McCormick, M., Di Cosmo, N., Sigl, M., Jungclaus, J., *et al.*, 2016. Cooling and societal change during the Late Antique Little Ice Age from 536 to around 660 AD. *Nature Geoscience* 9, 231–236.

Büntgen, U., Tegel, W., Nicolussi, K., McCormick, M., Frank, D., Trouet, V., Kaplan, J.O., *et al.*, 2011. 2500 Years of European climate variability and human susceptibility. *Science* 331, 578–582.

Burns, S.J., Matter, A., Frank, N., Mangini, A., 1998. Speleothem-based paleoclimate record from northern Oman. *Geology* 26, 499–502.

Chambers, F.M., Barber, K.E., Maddy, D., Brew, J., 1997. A 5500-year proxy-climate and vegetation record from blanket mire at Talla Moss, Borders, Scotland. *Holocene* 7, 391–399.

Charman, D.J., 2010. Centennial climate variability in the British Isles during the mid–late Holocene. *Quaternary Science Reviews* 29, 1539–1554.

Charman, D.J., Barber, K.E., Blaauw, M., Langdon, P.G., Mauquoy, D., Daley, T.J., Hughes, P.D.M., Karofeld, E., 2009. Climate drivers for peatland palaeoclimate records. *Quaternary Science Reviews* 28, 1811–1819.

Charman, D.J., Blundell, A., 2007. A new European testate amoebae transfer function for palaeohydrological reconstruction on ombrotrophic peatlands. *Journal of Quaternary Science* 22, 209–221.

Charman, D.J., Brown, A.D., Hendon, D., Karofeld, E., 2004. Testing the relationship between Holocene peatland palaeoclimate reconstructions and instrumental data at two European sites. *Quaternary Science Reviews* 23, 137–143.

Cheyette, F.L., 2008. The disappearance of the ancient landscape and the climatic anomaly of the early Middle Ages: a question to be pursued. *Early Medieval Europe* 16, 127–165.

Cook, E.R., Seager, R., Kushnir, Y., Briffa, K.R., Büntgen, U., Frank, D., Krusic, P.J., *et al.*, 2015. Old World megadroughts and pluvials during the Common Era. *Science Advances* 1, e1500561.

Dalton, C., Birks, H.J.B., Brooks, S.J., Cameron, N.G., Evershed, R. P., Peglar, S.M., Scott, J.A., Thompson, R., 2005. A multi-proxy study of lake-development in response to catchment changes during the Holocene at Lochnagar, north-east Scotland. *Palaeogeography, Palaeoclimatology, Palaeoecology* 221, 175–201.

Dreßler, M., Selig, U., Dörfler, W., Adler, S., Schubert, H., Hübener, T., 2006. Environmental changes and the Migration Period in northern Germany as reflected in the sediments of Lake Dudinghausen. *Quaternary Research* 66, 25–37.

Dugmore, A.J., Larsen, G., Newton, A.J., 1995. Seven tephra isochrones in Scotland. *Holocene* 5, 257–266.

Ervynck, A., Baeteman, C., Demiddele, H., Hollevoet, Y., Pieters, M., Schelvis, J., Tys, D., Van Strydonck, M., Verhaeghe, F., 1999. Human occupation because of a regression, or the cause of a transgression. A critical review of the interaction between geological events and human occupation in the Belgian coastal plain during the first millennium AD. *Probleme der Küstenforschung im südlichen Nordseegebiet* 26, 97–121.

Esper, J., Frank, D., Büntgen, U., Verstege, A., Luterbacher, J., Xoplaki, E., 2007. Long-term drought severity variations in Morocco. *Geophysical Research Letters* 34, L17702.

Fohlmeister, J., Schröder-Ritzrau, A., Scholz, D., Spötl, C., Riechelmann, D.F.C., Mudelsee, M., Wackerbarth, A., *et al.*, 2012. Bunker Cave stalagmites: an archive for central European Holocene climate variability. *Climate of the Past* 8, 1751–1764.

Forster, E.E., 2010. Palaeoecology of Human Impact in Northwest England during the Early Medieval Period: Investigating "Cultural Decline" in the Dark Ages. PhD dissertation, University of Southampton, Southampton, UK.

Frisia, S., Borsato, A., Mangini, A., Spötl, C., Madonia, G., Sauro, U., 2006. Holocene climate variability in Sicily from a discontinuous stalagmite record and the Mesolithic to Neolithic transition. *Quaternary Research* 66, 388–400.

Fuller, L., Baker, A., Fairchild, I.J., Spötl, C., Marca-Bell, A., Rowe, P., Dennis, P.F., 2008. Isotope hydrology of dripwaters in a Scottish cave and implications for stalagmite palaeoclimate research. *Hydrology and Earth System Sciences* 12, 1065–1074.

Galka, M., Miotk-Szpiganowicz, G., Goslar, T., Jesko, M., van der Knaap, W.O., Lamentowicz, M., 2013. Palaeohydrology, fires and vegetation succession in the southern Baltic during the last 7500 years reconstructed from a raised bog based on multi-proxy data. *Palaeogeography, Palaeoclimatology, Palaeoecology* 370, 209–221.

Geirsdóttir, Á., Miller, G.H., Axford, Y., Sadís, Ó., 2009. Holocene and latest Pleistocene climate and glacier fluctuations in Iceland. *Quaternary Science Reviews* 28, 2107–2118.

Gräslund, B., Price, N., 2012. Twilight of the gods? The "dust veil event" of AD 536 in critical perspective. *Antiquity* 86, 428–443.

Helama, S., Jones, P.D., Briffa, K.R., 2017a. Dark Ages Cold Period: a literature review and directions for future research. *Holocene* 27, 1600–1606.

Helama, S., Jones, P.D., Briffa, K.R., 2017b. Limited Late Antique cooling. *Nature Geoscience* 10, 242–243.

Kalis, A.J., Karg, S., Meurers-Balke, H., Teunissen-van Oorschot, H., 2008. Mensch und Vegetation am Unteren Niederrhein währen der Eisen- und Römerzeit. In: Müller, M., Schalles, H.-J., Zieling, N. (Eds.), *Colonia Ulpia Traiana, Xanten und sein Umland in römischer Zeit. Xantener Berichte. Geschichte der Stadt Xanten*. Verlag Philipp von Zabern, Mainz am Rhein, Germany, pp. 31–48.

Kottek, M., Grieser, J., Beck, C., Rudolf, B., Rubel, F., 2006. World map of the Köppen-Geiger climate classification updated. *Meteorologische Zeitschrift* 15, 259–263.

Kress, A., Saurer, M., Siegwolf, R.T.W., Frank, D.C., Esper, J., Bugmann, H., 2010. A 350 year drought reconstruction from Alpine tree ring stable isotopes. *Global Biogeochemical Cycles* 24, 1–16.

Lamentowicz, M., Cedro, A., Galka, M., Goslar, T., Miotk-Szpiganowicz, G., Mitchell, E.A.D., Pawlyta, J., 2008. Last millennium palaeoenvironmental changes from a Baltic bog (Poland) inferred from stable isotopes, pollen, plant macrofossils and testate amoebae. *Palaeogeography, Palaeoclimatology, Palaeoecology* 265, 93–106.

Lamentowicz, M., Mitchell, E.A.D., 2005. The ecology of testate amoebae (protists) in sphagnum in north-western Poland in relation to peatland ecology. *Microbial Ecology* 50, 48–63.

Langdon, P.G., Barber, K.E., Hughes, P.D.M., 2003. A 7500-year peat-based palaeoclimatic reconstruction and evidence for an 1100-year cyclicity in bog surface wetness from Temple Hill Moss, Pentland Hills, southeast Scotland. *Quaternary Science Reviews* 22, 259–274.

Langdon, P.G., Barber, K.E., Lomas-Clarke, S.H., 2004. Reconstructing climate and environmental change in northern England through chironomid and pollen analyses: evidence from Talkin Tarn, Cumbria. *Journal of Paleolimnology* 32, 197–213.

Larsen, L.B., Vinther, B.M., Briffa, K.R., Melvin, T.M., Clausen, H. B., Jones, P.D., Siggaard-Andersen, M.L., *et al.*, 2008. New ice core evidence for a volcanic cause of the A.D. 536 dust veil. *Geophysical Research Letters* 35, L04708.

Litt, T., Schölzel, C., Kühl, N., Brauer, A., 2009. Vegetation and climate history in the Westeifel Volcanic Field (Germany) during the past 11 000 years based on annually laminated lacustrine maar sediments. *Boreas* 38, 679–690.

Ljungqvist, F.C., 2009. Temperature proxy records covering the last two millenia: A tabular and visual overview. *Geografiska Annaler: Series A, Physical Geography* 91, 11–29.

Ljungqvist, F.C., 2010. A new reconstruction of temperature variability in the extra-tropical Northern Hemisphere during the last two millennia. Geografiska Annaler: Series A, *Physical Geography* 92, 339–351.

https://doi.org/10.1017/qua.2018.84 Published online by Cambridge University Press

Luterbacher, J., Werner, J.P., Smerdon, J.E., Fernández-Donado, L., González-Rouco, F.J., Barriopedro, D., Ljungqvist, F.C., *et al.*, 2016. European summer temperatures since Roman times. *Environmental Research Letters* 11, 024001.

Mangini, A., 2005. Assessing the variability of precipitation during the Holocene from stalagmite records. *Società Astronomica Italiana* 76, 755–759.

Mangini, A., Spötl, C., Verdes, P., 2005. Reconstruction of temperature in the Central Alps during the past 2000 yr from a $\delta^{18}O$ stalagmite record. *Earth and Planetary Science Letters* 235, 741–751.

McCormick, M., Büntgen, U., Cane, M.A., Cook, E.R., Harper, K., Huybers, P., Litt, T., *et al.*, 2012. Climate change during and after the Roman Empire: reconstructing the past from scientific and historical evidence. *Journal of Interdisciplinary History* 43, 169–220.

McDermott, F., Mattey, D.P., Hawkesworth, C., 2001. Centennial-scale Holocene climate variability revealed by a high-resolution speleothem $\delta^{18}O$ record from SW Ireland. *Science* 294, 1328–1331.

Ménot, G., Burns, S.J., 2001. Carbon isotopes in ombrogenic peat bog plants as climatic indicators: calibration from an altitudinal transect in Switzerland. *Organic Geochemistry* 32, 233–245.

Moschen, R., Kühl, N., Peters, S., Vos, H., Lücke, A., 2011. Temperature variability at Dürres Maar, Germany during the Migration Period and at High Medieval Times, inferred from stable carbon isotopes of *Sphagnum* cellulose. *Climate of the Past* 7, 1011–1026.

Moschen, R., Kühl, N., Rehberger, I., Lücke, A., 2009. Stable carbon and oxygen isotopes in sub-fossil *Sphagnum*: assessment of their applicability for palaeoclimatology. *Chemical Geology* 259, 262–272.

Niggemann, S., Mangini, A., Richter, D.K., Wurth, G., 2003. A paleoclimate record of the last 17,600 years in stalagmites from the B7 cave, Sauerland, Germany. *Quaternary Science Reviews* 22, 555–567.

Pierik, H.J., Cohen, K.M., Stouthamer, E., 2016. A new GIS approach for reconstructing and mapping dynamic late Holocene coastal plain palaeogeography. *Geomorphology* 270, 55–70.

Proctor, C., Baker, A., Barnes, W., 2002. A three thousand year record of North Atlantic climate. *Climate Dynamics* 19, 449–454.

Proctor, C.J., Baker, A., Barnes, W.L., Gilmour, M.A., 2000. A thousand year speleothem proxy record of North Atlantic climate from Scotland. *Climate Dynamics* 16, 815–820.

Rasmussen, S.O., Andersen, K.K., Svensson, A.M., Steffensen, J.P., Vinther, B.M., Clausen, H.B., Siggaard-Andersen, M.L., *et al.*, 2006. A new Greenland ice core chronology for the last glacial termination. *Journal of Geophysical Research: Atmospheres* 111, D06102.

Richards, D.A., Dorale, J.A., 2003. Uranium-series chronology and environmental applications of speleothems. *Reviews in Mineralogy and Geochemistry* 52, 407–460.

Riechelmann, D.F.C., Deininger, M., Scholz, D., Riechelmann, S., Schröder-Ritzrau, A., Spötl, C., Richter, D.K., Mangini, A., Immenhauser, A., 2013. Disequilibrium carbon and oxygen isotope fractionation in recent cave calcite: comparison of cave precipitates and model data. *Geochimica et Cosmochimica Acta* 103, 232–244.

Riechelmann, D.F.C., Schröder-Ritzrau, A., Scholz, D., Fohlmeister, J., Spötl, C., Richter, D.K., Mangini, A., 2011. Monitoring Bunker Cave (NW Germany): a prerequisite to interpret geochemical proxy data of speleothems from this site. *Journal of Hydrology* 409, 682–695.

Scholz, D., Hoffmann, D.L., 2008. $^{230}Th/U$-dating of fossil reef corals and speleothems. *Quaternary Science Journal (Eiszeitalter und Gegenwart)* 57, 52–77.

Sundqvist, H.S., Zhang, Q., Moberg, A., Holmgren, K., Körnich, H., Nilsson, J., Brattström, G., 2010. Climate change between the mid and late Holocene in the northern high latitudes. Part 1: survey of temperature and precipitation proxy data. *Climate of the Past* 6, 591–608.

Swindles, G.T., Lawson, I.T., Matthews, I.P., Blaauw, M., Daley, T. J., Charman, D.J., Roland, T.P., *et al.*, 2013. Centennial-scale climate change in Ireland during the Holocene. *Earth-Science Reviews* 126, 300–320.

Teunissen, D., 1990. Palynologisch onderzoek in het oostelijk rivierengebied: een overzicht. Mededelingen van de afdeling Biogeologie van de Discipline Biologie van de Katholieke Universiteit van Nijmegen, Nijmegen, the Netherlands.

Tinner, W., Lotter, A.F., Ammann, B., Conedera, M., Hubschmid, P., van Leeuwen, J.F.N., Wehrli, M., 2003. Climatic change and contemporaneous land-use phases north and south of the Alps 2300 BC to 800 AD. *Quaternary Science Reviews* 22, 1447–1460.

Tipping, R., 1995. Holocene evolution of a lowland Scottish landscape: Kirkpatrick Fleming. Part I, peat- and pollen-stratigraphic evidence for raised moss development and climatic change. *Holocene* 5, 69–81.

Toohey, M., Krüger, K., Sigl, M., Stordal, F., Svensen, H., 2016. Climatic and societal impacts of a volcanic double event at the dawn of the Middle Ages. *Climatic Change* 136, 401–412.

Toonen, W.H.J., 2013. A Holocene Flood Record of the Lower Rhine. PhD dissertation, Utrecht University, Utrecht, the Netherlands.

Vinther, B.M., Clausen, H.B., Johnsen, S.J., Rasmussen, S.O., Andersen, K.K., Buchardt, S.L., Dahl-Jensen, D., *et al.*, 2006. A synchronized dating of three Greenland ice cores throughout the Holocene. *Journal of Geophysical Research: Atmospheres* 111, D13102.

Vollweiler, N., Scholz, D., Mühlinghaus, C., Mangini, A., Spötl, C., 2006. A precisely dated climate record for the last 9 kyr from three high alpine stalagmites, Spannagel Cave, Austria. *Geophysical Research Letters* 33, L20703.

Wanner, H., Beer, J., Bütikofer, J., Crowley, T.J., Cubasch, U., Flückiger, J., Goosse, H., *et al.*, 2008. Mid- to late Holocene climate change: an overview. *Quaternary Science Reviews* 27, 1791–1828.

Wanner, H., Solomina, O., Grosjean, M., Ritz, S.P., Jetel, M., 2011. Structure and origin of Holocene cold events. *Quaternary Science Reviews* 30, 3109–3123.

Wickham, C., 2009. *The Inheritance of Rome: A History of Europe from 400 to 1000*. Penguin, New York.

Wilson, R., Anchukaitis, K., Briffa, K.R., Büntgen, U., Cook, E., D'Arrigo, R., Davi, N., Esper, J., Frank, D., Gunnarson, B., Hegerl, G., Helama, S., Klesse, S., Krusic, P.J., Linderholm, H. W., Myglan, V., Osborn, T.J., Rydval, M., Schneider, L., Schurer, A., Wiles, G., Zhang, P., Zorita, E., 2016. Last millennium northern hemisphere summer temperatures from tree rings: Part I: The long term context. *Quaternary Science Reviews* 134, 1–18.

Wilson, R.J.S., Luckman, B.H., Esper, J., 2005. A 500 year dendroclimatic reconstruction of spring–summer precipitation

https://doi.org/10.1017/qua.2018.84 Published online by Cambridge University Press

from the lower Bavarian Forest region, Germany. *International Journal of Climatology* 25, 611–630.

Woodland, W.A., Charman, D.J., Sims, P.C., 1998. Quantitative estimates of water tables and soil moisture in Holocene peatlands from testate amoebae. *Holocene* 8, 261–273.

Zolitschka, B., 1998. *Paläoklimatische Bedeutung laminierter Sedimente*. Gebr. Borntraeger, Berlin.

Zolitschka, B., Brauer, A., Negendank, J.F.W., Stockhausen, H., Lang, A., 2000. Annually dated late Weichselian continental paleoclimate record from the Eifel, Germany. *Geology* 28, 783–786.

https://doi.org/10.1017/qua.2018.84 Published online by Cambridge University Press